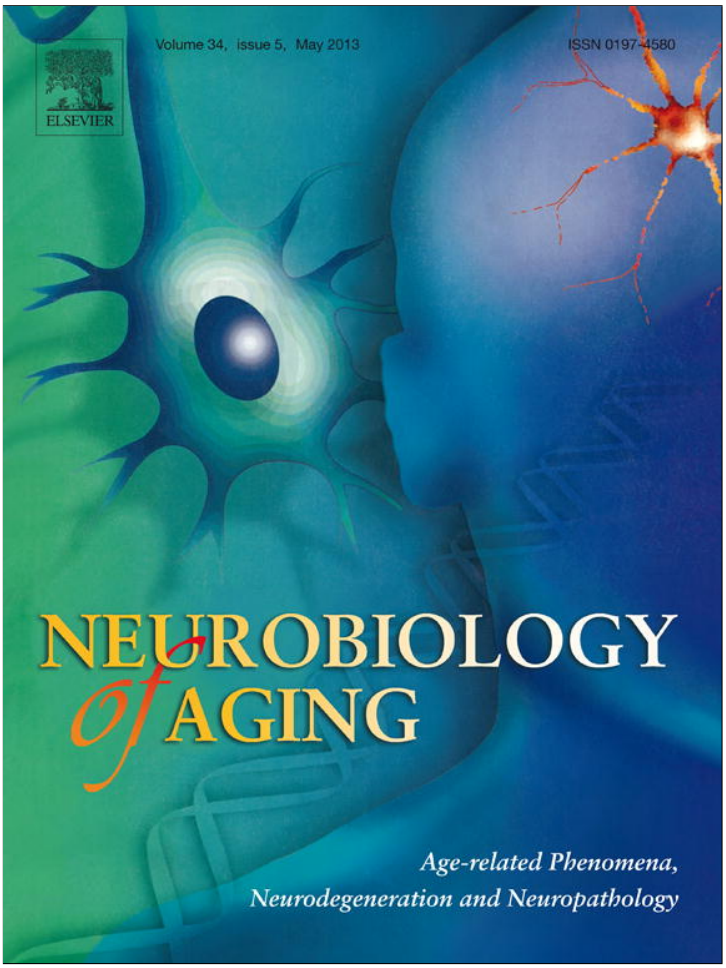

Neurobiology of Aging 34 (2013) 1469–1485

Contents lists available at SciVerse ScienceDirect

Neurobiology of Aging

journal homepage: www.elsevier.com/locate/neuaging

Age dependence of hemodynamic response characteristics in human functional magnetic resonance imaging

Claudine J. Gauthier [a,b,*], Cécile Madjar [b], Laurence Desjardins-Crépeau [b,c], Pierre Bellec [b,d], Louis Bherer [b,c], Richard D. Hoge [a,b]

[a] Physiology/Biomedical Engineering, Université de Montréal, Montreal, Quebec, Canada
[b] CRIUGM, Montreal, Quebec, Canada
[c] Psychology Department, UQAM, Montreal, Quebec, Canada
[d] Computer Science and Operations Research, Université de Montréal, Montreal, Quebec, Canada

ARTICLE INFO

Article history:
Received 22 July 2012
Received in revised form 1 October 2012
Accepted 2 November 2012
Available online 6 December 2012

Keywords:
Cognitive aging
Calibrated fMRI
Hypercapnia
Vascular reactivity
BOLD signal biases
Cerebral blood flow
Oxidative metabolism
Modified Stroop task

ABSTRACT

Functional magnetic resonance imaging (fMRI) studies of cognitive aging have generally compared the amplitude and extent of blood oxygen level-dependent (BOLD) signal increases evoked by a task in older and younger groups. BOLD is thus used as a direct index of neuronal activation and it is assumed that the relationship between neuronal activity and the hemodynamic response is unchanged across the lifespan. However, even in healthy aging, differences in vascular and metabolic function have been observed that could affect the coupling between neuronal activity and the BOLD signal. Here we use a calibrated fMRI method to explore vascular and metabolic changes that might bias such BOLD comparisons. Though BOLD signal changes evoked by a cognitive task were found to be similar between a group of younger and older adults (e.g., 0.50 ± 0.04% vs. 0.50 ± 0.05% in right frontal areas), comparison of BOLD and arterial spin labelling (ASL) responses elicited in the same set of structures by a controlled global hypercapnic manipulation revealed significant differences between the 2 groups. Older adults were found to have lower responses in BOLD and flow responses to hypercapnia (e.g., 1.48 ± 0.07% vs. 1.01 ± 0.06% over gray matter for BOLD and 24.92 ± 1.37% vs. 20.67 ± 2.58% for blood flow), and a generally lower maximal BOLD response *M* (5.76 ± 0.2% vs. 5.00 ± 0.3%). This suggests that a given BOLD response in the elderly might represent a larger change in neuronal activity than the same BOLD response in a younger cohort. The results of this study highlight the importance of ancillary measures such as ASL for the correct interpretation of BOLD responses when fMRI responses are compared across populations who might exhibit differences in vascular physiology.

1. Introduction

Aging is associated with a variety of changes in the brain. Though atrophy and white matter lesions are observable at the later stages in life (Brown et al., 2011; Salat et al., 2004), functional changes can also be observed (Chen et al., 2011; Lu et al., 2011). The effect of aging on the blood oxygen level-dependent (BOLD) signal evoked by a variety of tasks has been the subject of intense research in recent years and typical patterns of change are starting to emerge. Though several theories have been put forward to categorize and explain these patterns (Cabeza, 2002; Davis et al., 2008; Park and Reuter-Lorenz, 2009; Reuter-Lorenz and Cappell, 2008; Reuter-Lorenz and Park 2010; Schneider-Garces et al., 2010), the complexity of the age-related changes observed indicate that there might be several mechanisms at play (Cabeza et al., 2005; Reuter-Lorenz and Park 2010). One of the most frequently observed pattern of change is a decreased lateralization of frontal BOLD responses, often detected as a decreased left frontal activation but an increased right frontal BOLD signal increase in older participants (Cabeza, 2002; Reuter-Lorenz and Park 2010). These differences in BOLD signal patterns have typically been explained by some form of compensatory neuronal activity in older participants to counterbalance the effects of loss of function and decreased primary perception or processing capacity (Cabeza, 2002; Cabeza et al., 2005; Davis et al., 2008; Park and Reuter-Lorenz, 2009; Reuter-Lorenz and Cappell, 2008; Reuter-Lorenz and Park 2010). Implied in this type of theory is the fact that the additional recruitment should provide an advantage in terms of reduced age-related effects, usually observed as lower error rates or faster reaction times.

* Corresponding author at: 4565 Queen Mary, Montreal, Quebec H3W 1W5, Canada. Tel.: +1 514 340 2800 ×4120; fax: +1 514 340 3548.
E-mail address: claudine.gauthier@umontreal.ca (C.J. Gauthier).

0197-4580/$ – see front matter © 2013 Elsevier Inc. All rights reserved.
http://dx.doi.org/10.1016/j.neurobiolaging.2012.11.002

However, most of the results used to devise these theories are based on hemodynamic imaging techniques, with BOLD contrast at the forefront. Therefore, one of the main sources of potential confounds in functional magnetic resonance imaging (fMRI) studies of aging stems from the ambiguous nature of the BOLD signal, which makes it difficult to draw physiologically specific conclusions from the amplitude and spatial extent of observed changes. The increases in BOLD signal observed during tasks arise from concomitant local changes in blood flow, blood volume, and oxidative metabolism. This complicates the direct, quantitative comparison of BOLD signal changes between groups, especially when changes in hemodynamic function across groups are suspected (Ances et al., 2009; Chen et al., 2011; Lu et al., 2011; Mohtasib et al., 2012; Samanez-Larkin and D'Esposito, 2008). Because BOLD can only be expressed as a fractional change from an unknown baseline, differences in the extent or amplitude of the BOLD signal might simply reflect an altered baseline state rather than a change in neuronal activity. For example, a similar metabolic change or vascular response from a lower metabolic or cerebral blood flow (CBF) baseline could artificially inflate the BOLD response.

Changes in BOLD signal might also reflect a decreased vascular reactivity (Lu et al., 2011). Aging is known to be associated with hardening of blood vessels throughout the body (Brown and Thore, 2011; O'Rourke and Hashimoto, 2007). Increased rigidity in vessels of the brain could lead to a decreased vascular response to a given metabolic demand. This would then result in a lower BOLD signal change in older individuals with neuronal activity levels similar to those seen in younger individuals. All these potential sources of confounds make the interpretation of BOLD signal comparisons between groups more difficult. However, some of these difficulties in interpretation could be alleviated by obtaining more physiologically-specific signals. The framework of calibrated fMRI, in which ASL and controlled vascular manipulations are added to BOLD, might be ideal for this because the end result and intermediate steps can be informative in determining the sources of age-related changes in hemodynamic properties (Gauthier et al., 2012).

Calibrated fMRI techniques allow quantitative comparisons between groups by isolating the oxidative metabolic component of the BOLD response to a task, which can be expressed as the percent change in cerebral metabolic rate of O_2 consumption ($CMRO_2$) (Blockley et al., 2012; Chiarelli et al., 2007; Davis et al., 1998; Gauthier and Hoge, 2012a). The most widely adopted techniques have used respiratory manipulations to determine the change in BOLD signal produced by a controlled vascular challenge. The gas manipulations used have included hypercapnia (Davis et al., 1998; Hoge et al., 1999a) (breathing increased concentrations of CO_2), hyperoxia (Chiarelli et al., 2007) (breathing increased concentrations of O_2), or a combination of both (Gauthier and Hoge, 2012a; Gauthier et al., 2011). Hyperoxia increases the O_2 content of blood, and hypercapnia leads to large and well characterized changes in blood flow throughout gray matter from the vasodilatory properties of CO_2. Both these manipulations give rise to substantial increases in BOLD signal throughout the brain that can, in combination with quantification of the concomitant CBF change evoked, be used to characterize the vascular component of the BOLD signal (Goode et al., 2009; Hoge et al., 1999b; Ito et al., 2008; Mark et al., 2010; Stefanovic et al., 2006; Tancredi et al., 2012). More specifically, calibrated fMRI experiments use the CBF and BOLD response to a gas manipulation to estimate the maximum possible BOLD signal change, M. This calibration factor M corresponds to the BOLD signal that would be obtained from complete elimination of deoxygenated hemoglobin from cerebral veins. When this vascular component is estimated, it can be factored out of the BOLD response evoked by an experimental task, to yield an estimate of the $CMRO_2$ component of the task-evoked BOLD signal change measured. We have recently described an extension of previous models (Chiarelli et al., 2007; Davis et al., 1998) that takes into account arbitrary changes in both blood flow and oxygen content (Gauthier and Hoge, 2012a). This model will be used here to more accurately take into account blood flow and oxygenation changes caused by breathing manipulation.

In the present study, we have used hypercapnically calibrated fMRI to investigate the effects of aging on the different components of the hemodynamic response, in the context of a cognitive task that has often been used to assess age-related cognitive deficits. Several studies have reported a larger Stroop effect (increases in reaction time and error rates to conflicting textual cues) and task switching cost in older compared with younger adults (DiGirolamo et al., 2001; Jimura and Braver, 2010; Langenecker et al., 2004; Milham et al., 2002; Mohtasib et al., 2012; Prakash et al., 2011; Wasylyshyn et al., 2011; Yun et al., 2011; Zysset et al., 2007). A modified Stroop task previously used by our group (Gauthier et al., 2012) and involving an element of interference and of switching is used here to identify the brain regions in which age-related effects might be expected. This study therefore investigates the effects of two functional challenges: the modified Stroop task, which is typical of cognitive tasks that might be explored in a BOLD aging study, and a hypercapnic respiratory manipulation. The combination of acquisitions during these two functional challenges is used to investigate possible biases and confounds associated with BOLD studies of cognitive aging. Calibrated fMRI is used to estimate a number of vascular and metabolic parameters that jointly determine the final BOLD signal compared between young and old in typical fMRI studies of aging. These parameters might be used to assess the validity of direct BOLD signal comparisons between age groups. Because baseline blood flow and vascular reactivity are both expected to decrease with age (Chen et al., 2011; Lu et al., 2011), it might be that the maximal BOLD signal change is lower in older individuals, leading to bias in the interpretation of age-related BOLD signal differences.

2. Methods

2.1. Participants

Acquisitions were conducted in 31 young (10 female, with mean age of 24 ± 3 years) and 31 older (14 female, with mean age of 64 ± 5 years) healthy participants on a Siemens TIM Trio 3T magnetic resonance imaging (MRI) system (Siemens Medical Solutions, Erlangen, Germany) using the vendor-supplied 32-channel receive-only head coil for all acquisitions. All subjects gave informed consent and the project was approved by the local ethics committee (Comité mixte d'éthique de la recherche du Regroupement Neuroimagerie/Québec).

Exclusion criteria for this study included claustrophobia, cardiac disease, hypertension or taking blood pressure lowering medication, neurological or psychiatric illness, smoking, excessive drinking (more than 2 drinks per day), thyroid disease, diabetes, asthma, and using a regular treatment known to be vasoactive or psychoactive. Participants were all nonsmokers and older participants had all been nonsmokers for at least 5 years. Additionally, every participant had a fasting blood draw on the morning of the magnetic resonance acquisition day to ensure that their fasting blood glucose and cholesterol levels were normal, and older participants met with a geriatric MD to ensure that they did not meet any of the exclusion criteria for the study.

All participants completed a short neuropsychological screening battery to assess verbal reasoning (Similarities subtest of the Wechsler Adult Intelligence Scale III; WAIS-III) (Wechsler, 1997), short-term memory (Digit span forward of WAIS-III), working

memory (Digit span backward of WAIS-III), psychomotor speed (Digit Symbol of WAIS-III), attention, and executive functions (Trail Making Test, Part A and B, and Color-Word Interference Test of the Delis–Kaplan Executive Function System) (Delis, 2001; Reitan, 1958). Older adults participants also completed the Mini Mental State Examination (Folstein et al., 1975) to screen for global cognitive decline. Participants who scored less than 26 on the Mini Mental State Examination were excluded. None of the participants was excluded based on this criterion. Table 1 shows the mean scores for each test in both groups. The results are within the normal range of performance for all clinical tests.

Whenever possible, participants needing eyesight correction were asked to wear contact lenses on the day of the MRI experiment. For those without contact lenses, eyesight was corrected to the nearest possible 0.50 D using MRI-compatible glasses for the modified Stroop acquisition only. For participants with significant hearing losses, written instructions were projected onto a screen at the end of the bore that could be seen by participants through a mirror.

2.2. Magnetic resonance image acquisition

Sessions included 2 anatomical, 1 mm^3 magnetization prepared rapid gradient echo (MPRAGE) acquisitions with repetition time (TR)/echo time (TE)/flip angle = 2300 ms/3 ms/9°, 256 × 240 matrix, and a generalized autocalibrating partially parallel acquisition (GRAPPA) acceleration factor of 2 (Griswold et al., 2002). Older participants had an additional fluid attenuated inversion recovery (FLAIR) acquisition to estimate the presence and severity of white matter lesions. FLAIR acquisition parameters included TR/TE/flip angle = 9000 ms/107 ms/120 with echo train length of 15, an inversion time of 2500 ms, 512 × 512 matrix for an in-plane resolution of 0.43 × 0.43 mm and 25 slices of 4.8 mm. White matter hyperintensities were quantified using the scale from Wahlund and colleagues (Wahlund et al., 2001). Only participants with scores of 0 or 1, corresponding to no or few small lesions, were included in this study. The score average and standard deviation was 0.67 ± 0.48 in the older group.

Functional image series were acquired using a dual-echo pseudo-continuous arterial spin labeling acquisition (Wu et al., 2007) to measure simultaneously changes in CBF and BOLD signal. The parameters used include: TR/TE 1/TE 2/flip angle = 3000 ms/10 ms/30 ms/90° with 4 × 4 mm in-plane resolution and 11 slices of 7 mm (1 mm slice gap) on a 64 × 64 matrix (at 7/8 partial Fourier), GRAPPA acceleration factor = 2, postlabeling delay = 900 ms, label offset = 100 mm, Hanning window-shaped right frontal pulse with duration/space = 500 μs/360 μs, flip angle of labeling pulse = 25°, slice-selective gradient = 6 mT/m, tagging duration = 1.5 seconds (Wu et al., 2007).

Imaging sessions were divided into in two parts. During one part, an MPRAGE, FLAIR, and modified Stroop functional acquisition was acquired. During the other, an MPRAGE and the hypercapnia functional acquisition was performed. Participants were taken out of the scanner in between these two acquisition segments to either put on, or take off the hypercapnia mask depending on the order of acquisitions. Participants were allowed to move or stretch during this pause to ensure greater comfort, especially in the older participants.

Table 1
Neuropsychological battery results

	Younger	Older
Sex (M/F)	21/10	17/14
Age	23.74 ± 0.52	63.53 ± 0.87
Education (y)	17.03 ± 0.38	16.01 ± 0.57
MMSE (score)	—	28.81 ± 0.20
Similarities (score)	26.16 ± 0.86	23.69 ± 0.85
Digit span forward (score)	9.87 ± 0.41	10.69 ± 0.40
Digit span backward (score)	7.39 ± 0.41	7.06 ± 0.40
Digit symbol (score)	92.48 ± 2.13	66.09 ± 2.32
CWIT – Color naming (s)	25.65 ± 0.74	29.65 ± 0.94
CWIT – Reading (s)	19.15 ± 0.49	20.23 ± 0.64
CWIT – Inhibition (s)	41.89 ± 1.33	57.12 ± 2.22
CWIT – Switching (s)	49.46 ± 2.14	58.33 ± 3.71
TMT – Part A (s)	26.00 ± 1.45	34.15 ± 1.65
TMT – Part B (s)	56.55 ± 3.66	78.45 ± 5.14

This table shows the average ± standard error in each group for all tests included in the battery administered to participants. The results are within the normal range of performance for all clinical tests.
Key: CWIT, Color-Word Interference Test; F, female; M, male; MMSE, Mini Mental State Examination; TMT, Trail Making Test.

2.3. Hypercapnic manipulation

Hypercapnic manipulations were achieved using a computer-controlled gas delivery system in combination with a sequential gas delivery circuit (RespirAct; Thornhill Research Inc, Toronto, Ontario, Canada). The RespirAct system allows independent control of end-tidal partial pressure of CO_2 (PCO_2) and end-tidal partial pressure of O_2 (PO_2) using a feed-forward physiological model, using as input the measured or predicted baseline O_2 consumption and CO_2 production of a subject (Slessarev et al., 2007). PCO_2 was targeted to be 40 mm Hg at baseline and 45 mm Hg during the hypercapnia blocks. PO_2 was targeted to be 100 mm Hg throughout the experiment. Gas was sampled continuously at the mouth and analyzed for PCO_2 and PO_2. RespirAct software calculated PCO_2 and PO_2 from the continuous partial pressure data. These calculations were confirmed manually in post hoc analysis. During the hypercapnic stimulation, volunteers breathed through the circuit via a soft plastic mask sealed to the face using adhesive dressing (Tegaderm 3M Healthcare, St. Paul, MN, USA), as necessary to prevent gas leakage. Participants were asked to breathe deeply enough to empty the fresh gas compartment of the breathing circuit at every breath during the functional acquisitions (to ensure delivery of the entire gas dose delivered by the machine). Generally, subjects did not have difficulty complying with this requirement.

Participants underwent the manipulation twice during the study, once outside the scanner before the imaging session to acclimatize the participant to the manipulation and once during the MRI session. Subjects were interviewed after the acclimatization session to assess their level of respiratory discomfort using the 7-point scale published by Banzett and colleagues (Banzett et al., 1996). Subjects reporting subjective rating of 5 or greater (significant discomfort) were not invited to continue in the study (2 cases).

2.4. Stroop task

The Stroop task (Gauthier et al., 2012) consisted of two 60-second blocks each of control and Stroop conditions, interspersed with 60-second rest blocks. In total, there were 4 task and 5 resting blocks, for a total acquisition length of 9 minutes (Fig. 1). During task blocks, control or Stroop events always lasted 2.5 seconds, preceded by 1.5 seconds with a fixation cross to maintain a constant gaze direction. The task was presented and the responses recorded using the Eprime software (version 1.2; Psychology Software Tools, Inc, Sharpsburg, PA, USA). The task was presented to participants using an LCD projector (EMP-8300; Epson, Toronto, Ontario, Canada) onto a translucent screen viewed by subjects through a mirror integrated into the Siemens head coil. In all cases, subjects had only 2 possible answers (blue or green), selected using an MRI-compatible button box (FIU-005 interface with 8 buttons bimanual response pads, Current Designs, Philadelphia, PA, USA). Most subjects were native French speakers or had been speaking French

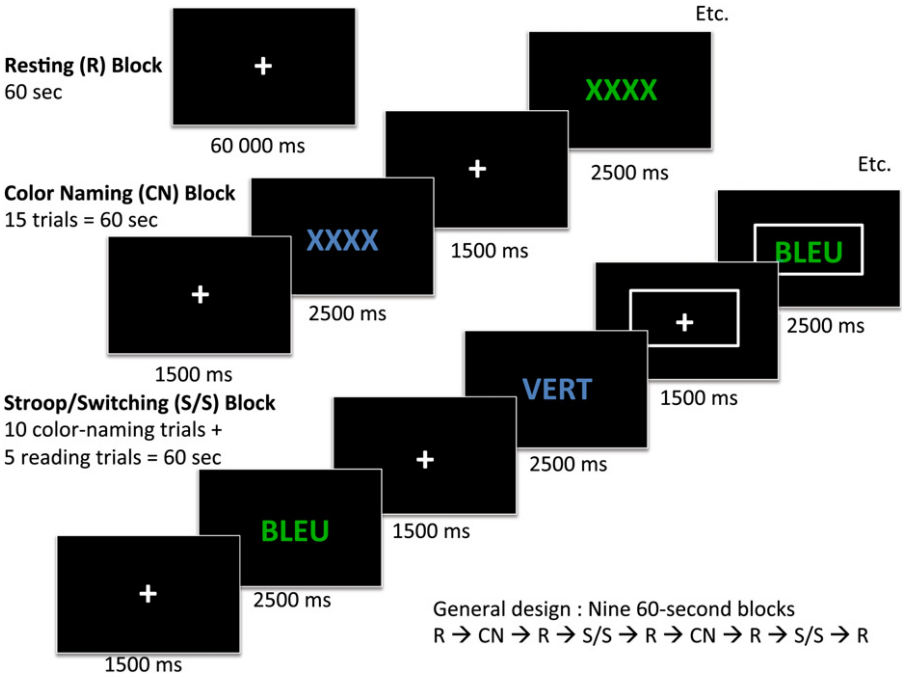

Fig. 1. Modified Stroop task diagram. This figure shows the different task conditions and block order of the modified Stroop task used during functional acquisition.

on a daily basis for more than 30 years and the color words were written in French ('BLEU' and 'VERT'). An English version of this task was also available for native English speakers (two in the younger and one in the older group).

During the Stroop/switching condition blocks, two different types of events were given in random order. In all cases, letter color and word semantic were noncongruent. In 10 of 15 cases, when the color word appeared, the correct answer was letter color. In 5 cases out of 15, a large white rectangle appeared around the word for the whole event, starting during the 2 seconds with the fixation cross. This rectangle indicated to the subject that the rule had changed and that the right answer now corresponded to word semantic rather than letter color. During the control task blocks (color naming), a series of 4 X's were written either in blue or green and the participant was asked to give the color of the letters.

2.5. Data analysis

All analyses except for group analysis, definition of Stroop regions of interest (ROIs), and registration of images to the MNI152 template were done using the NeuroLens data analysis software package (www.neurolens.org). All raw echo planar imaging (EPI) series were preprocessed by motion correction (Cox and Jesmanowicz, 1999) and spatial smoothing with a 3-D Gaussian kernel (6 mm full width half maximum). The CBF signal was isolated from the series of first echoes using linear surround subtraction (Liu and Wong, 2005), and the BOLD signal was extracted using linear surround addition of the second echo series (Gauthier and Hoge, 2012b; Gauthier et al., 2012; Liu and Wong, 2005).

Fractional changes in BOLD and CBF signals were then determined for hypercapnia by fitting a general linear model (GLM) to the respective signals and dividing the estimated effect size by the estimated constant term. Model fits used a single-gamma hemodynamic response function with parameters described by Glover (1999) and included linear, quadratic, and third order polynomials to represent baseline signal and drifts. CBF and BOLD data for the Stroop task were treated similarly. For the Stroop task, a contrast was used to isolate the signal changes during the inhibition/switching blocks. Temporal signal-to-noise ratio (tSNR) maps were derived from the CBF and BOLD datasets for the modified Stroop task. These were obtained by dividing the β of the linear baseline term by the residuals from the GLM at each voxel. The tSNR represents the ratio between the baseline functional signal and the temporal fluctuations arising from hardware thermal noise and physiological sources of fluctuations (Kruger and Glover, 2001; Triantafyllou et al., 2005).

The average time course for CBF and BOLD of both hypercapnia and modified Stroop tasks were determined using a finite impulse response (FIR) analysis, which is a parsimonious method for averaging blocked responses within the context of a GLM fit that can be used to remove spurious drift terms. For purposes of the FIR fit, the 'events' were defined as being the block onsets, shifted earlier in time as needed to capture a brief interval of baseline before the task block. The number of FIR regressors was then chosen to adequately cover the initial baseline period, the task block, and a brief period after the task block. Using this approach, the temporal response was measured for 15 seconds before the beginning and after the end of each block (either hypercapnia or modified Stroop), to capture the rising, plateau, and descending phases of the response. All other parameters were as in the previously described GLM analysis. The time course amplitudes of the regressor of interest (hypercapnia or modified Stroop) were divided by the baseline term from the GLM to obtain the time course in units of percent change CBF or BOLD. Individual time courses were averaged over all subjects in each group. To facilitate comparisons between groups and because the FIR trace does not always have an initial baseline of 0 as expected, the first 5 TRs (−15 seconds to 0) were averaged and the whole trace was shifted by this average offset to bring the traces to a baseline of 0.

Absolute resting CBF was determined from the pseudocontinuous arterial spin labeling data using the approach described by Wang et al. (2003) assuming blood–brain partition coefficient = 0.9, labeling efficiency = 0.80, blood T1 = 1.49 seconds, and gray matter T1 = 1.4 seconds. For this computation, the baseline ASL difference signal estimated in the GLM fit for each gas manipulation was divided by the corresponding unsubtracted baseline EPI signal from the ASL series, computed in a similar GLM fit carried out on

the unsubtracted EPI series. The unsubtracted baseline EPI signal from the ASL series is used here as a surrogate for the fully relaxed magnetization that can alternately be acquired in the form of what is termed an M_0 scan. To account for incomplete recovery of longitudinal magnetization during the sequence TR of 3 seconds, baseline EPI estimates from gray matter ROIs were corrected using the gray matter T1 value cited above. The resultant ratio was converted to absolute CBF units based on the parameters above. Cerebrovascular reactivity was obtained by dividing the percent BOLD and CBF signal changes during the hypercapnia manipulation by the increase in end-tidal PCO_2 values during this manipulation (Forbes et al., 1997; Gauthier et al., 2012; Graham et al., 1994).

The generalized calibration model (GCM) method was used as by Gauthier and Hoge, (2012a), Gauthier et al. (2012) to obtain *M* estimates for each subject. Under the conditions of this study, the results should be very similar to those obtained using the hypercapnia calibration model (Davis et al., 1998). Small differences might arise if arterial saturation is estimated to be less than 100% (Gauthier and Hoge, 2012a), but saturation values are expected to be very high in healthy individuals. Evoked $CMRO_2$ values were obtained using group average values for all input parameters (percent CBF and BOLD change during the modified Stroop task and *M* value). One older participant was excluded from this analysis because their CBF response to CO_2 and the modified Stroop task were found to be outliers.

ROI quantification was done by weighted averaging of voxels in EPI space, taking into account the gray matter volume fraction from automated tissue segmentation (described in the next section) at each voxel. All uncertainties are provided as ± standard error. Uncertainties on evoked $CMRO_2$ were computed from propagation of uncertainties on *M*, CBF, and BOLD as described in Davis et al. (1998).

2.6. ROIs definition

ROIs were defined independently for each age group using their respective areas of significant signal changes in the group analysis maps. Group analyses and normalization for ROI definition were done using FSL (version 4.1.9). All functional data were motion corrected with MCFLIRT (Jenkinson et al., 2002) and the brain was extracted using Brain Extraction Tool (version 2.1) (Smith, 2002). A 6 mm^3 full width half maximum 3-D Gaussian smoothing kernel, high-pass filter (100-second cutoff) and prewhitening (Woolrich et al., 2001) were applied to the time series. Spatial normalization to standard space (MNI152 template) (Jenkinson and Smith, 2001; Jenkinson et al., 2002) was performed (12 *df*) on the 30 ms echo time series. Spatial transformation matrices for the 30 ms echo time series were used for the 10 ms time series, to minimize normalization errors from the bright scalp signal in the shorter echo. The flow-dependent component of the first echo time series (TE = 10 ms) was isolated through sinc interpolation subtraction between neighboring points. The BOLD time series was extracted from the second echo time series (TE = 30 ms) by isolating the control images from the original time series. A GLM was performed with the main experimental paradigm convolved with a dual gamma function. Temporal derivatives were included in the model. Mixed effect group analysis was performed using FLAME1 (Beckmann et al., 2003; Woolrich, 2008; Woolrich et al., 2004) to generate group average statistical maps for the contrast representing the significant BOLD signal increases during the inhibition/switching blocks. The intersection of group average maps with Gaussian random field voxel-wise thresholding corrected at $p = 0.01$ for each echo (i.e., the intersection of signifiant CBF and BOLD peaks) was used to derive the individual ROIs. Four ROIs were drawn using the map of the intersection of significant BOLD and ASL maps for the group (Fig. 1). Two ROIs focused on significant activation over left and right frontal areas. A third ROI was drawn over significantly activated bilateral parietal areas. Because changes in laterality of activations is predominantly discussed in the context of frontal BOLD signal changes in the literature (Cabeza, 2002; Cappell et al., 2010; Park and Reuter-Lorenz, 2009; Reuter-Lorenz and Park, 2010), only the frontal component of the activation was separated in lateral ROIs. The fourth ROI was derived from automated tissue segmentation of all gray matter. The transformation matrix used to register individual functional acquisitions to Montreal Neurological Institute space was inverted and this inverted transform was applied to each ROI derived from the group activation map to obtain ROIs in native space using linear interpolation.

To account for the fact that our large EPI voxels inevitably contained a mixture of gray matter, white matter, and cerebrospinal fluid, average BOLD and ASL responses were determined by computing weighted averages within ROIs, with the weighting provided by the estimated gray matter volume fraction in each voxel. The gray matter volume fraction was determined using automatic tissue segmentation of anatomic images using the FAST module of FSL (Zhang et al., 2001). Gray matter probability maps generated by FAST were projected into native EPI space using linear interpolation. Binarized individual ROI maps (Stroop task-derived) were multiplied by gray matter probability. This approach assumes that the responses in white matter and cerebrospinal fluid are negligible compared with the gray matter response, which is supported by our observations in these tissue compartments (data not shown).

2.7. Statistical analysis

Statistical analysis of the Stroop behavioral data was done using an analysis of variance as implemented in the SPSS 19.0 software (IBM, Armonk, NY, USA). The inhibition/switching cost was calculated by dividing the difference in reaction time between the inhibition/switching and control conditions by the reaction time of the control task.

The difference between age groups across physiological measure, functional challenge, and ROIs was tested using a general linear model analysis, as implemented in the Neuroimaging Analysis Kit (http://www.nitrc.org/projects/niak). First, the effect of age was investigated using a model pooling the measures from all the ROIs. The purpose of this model was to test the overall effect of age across all the ROIs, regardless of its significance at any particular ROI. The explanatory variables of the model included a dummy variable coding for the age group of each subject. In addition, the differences between the mean value for each of the 4 ROIs were coded using an intercept and 3 dummy variables, following the method described by Gujarati (2002). The intercept captured the mean across all 4 ROIs. The first variable dummy variable coded for the difference between the mean of ROI 1 (gray matter) and the mean of ROI 2–4 (left and right frontal, and parietal). The second dummy variable coded for the difference between the mean of ROIs 1 and 2 and the mean of ROIs 3 and 4. The third dummy variable coded for the difference between the mean of ROIs 1–3 and the mean of ROI 4. The significance level of the overall effect of age across all regions was corrected for multiple comparisons across contrasts and experiments using Bonferroni's procedure (significance threshold p of 0.05 divided by 11 types of estimation, $p = 0.0045$). For combinations of physiological measure/functional challenge in which age had an overall effect across ROIs, we further tested the significance of age effects at each ROI. This means that for each ROI, we used a reduced model including only the measurements coming from this ROI, and an intercept and age groups coded as a dummy variable for explanatory variables. The significance of the effect of age for each region was corrected for multiple

comparisons across ROIs using the Bonferroni procedure (significance threshold p of 0.05 divided by 4 ROIs, $p = 0.0125$). We did not correct for multiple comparisons across physiological measure/functional challenge at this level, because we already assumed that the omnibus test for the overall effect of age was significant for this particular combination of physiological measure/functional challenge.

3. Results

3.1. Modified Stroop task behavioral results

This study explores the hemodynamic and vascular changes in regions implicated in a modified Stroop task (Fig. 1) thought to be associated with age-related changes. Reaction times and error rates were found do be significantly higher in the older group, during the control and during the inhibition/switching blocks ($p < 0.0001$). Reaction times during the control block were 575.52 ± 25.14 ms and 696.78 ± 19.63 ms in younger and older adults for the control task, and 898.20 ± 38.08 ms and 1239.91 ± 34.26 ms for the inhibition/switching blocks in younger and older adults, respectively (Fig. 2A). The group by condition interaction ($p < 0.0001$) showed that the reaction time increase from the inhibition/switching compared with control condition was larger in older than younger adults. The cost in terms of reaction time for the inhibition/switching condition was 56.07 ± 4.92% and 77.95 ± 4.67% for the younger and older adults respectively, indicating a larger age-related slowing for inhibition/switching beyond the general slowing seen with age. A significant group by condition interaction was also observed in accuracy ($p = 0.007$) (Fig. 2B) with older adults showing a larger decline in accuracy in the switching condition. Percent correct responses in younger and older adults respectively for the control task were 99.52 ± 0.24% and 97.58 ± 1.61%. Accuracy during the inhibition/switching blocks was 96.19 ± 0.82% and 87.39 ± 2.41% in the younger and older groups respectively.

3.2. Modified Stroop activation maps

Group analysis of the inhibition/switching blocks revealed significant BOLD and ASL signal increases in similar areas for both groups. Significant BOLD and ASL increases (Fig. 3) were found in several regions of cortex including anterior cingulate, part of the frontal, parietal, and occipital lobes, and some subcortical structures covering mainly the putamen. Frontal activation foci were bilateral and covered part of the middle frontal and inferior frontal gyri. This area of activation also extended partially over precentral gyrus. Activation over parietal areas was extensive, covering areas 40 and 7 and extending down into occipital areas.

However, no significant difference was detected in a group average map for the contrast old minus young, for either the CBF or BOLD data. ROIs were drawn over the frontal and parietal areas significantly activated within each group during the inhibition/switching blocks (Fig. 4). Responses within these ROIs are discussed below.

3.3. Stroop evoked responses

Percent BOLD and CBF responses to the inhibition/switching blocks of the modified Stroop task were quantified in 3 ROIs: left frontal, right frontal, and parietal areas. BOLD response amplitude during the task was similar ($p = 0.85$) between the 2 groups (Fig. 5A and Table 2). Percent BOLD signal responses quantified over individual ROIs are shown in Fig. 5A and Table 2.

ASL data shows a somewhat different picture, with a significant general age effect ($p < 0.0001$) (Fig. 5B and Table 2). Percent changes have been converted to absolute increase in CBF, in units of mL/100 g/min for each individual using ROI-average value of resting blood flow for this comparison. The values in percentage, which are used as input into the calibrated fMRI model are shown in Table 2. CBF responses were similar between the two groups in the left frontal ROI ($p = 0.26$), and right frontal ROI showed higher responses in the older group ($p = 0.002$). Finally, the parietal CBF change showed a trend toward higher responses in the older group ($p = 0.04$, threshold to account for multiple comparisons of $p = 0.013$).

3.4. Respiratory manipulation

The hypercapnia protocol led to the expected increase in CO_2, with stable plateaus within a few breaths. End-tidal values were increased by 4.81 ± 0.15 mm Hg in the younger group and 4.49 ± 0.21 mm Hg in the older group, from baseline values of 38.50 ± 0.23 mm Hg and 39.31 ± 0.33 mm Hg in the younger and older groups respectively. End-tidal CO_2 change between the baseline and the hypercapnia block did not differ significantly between the two groups. End-tidal O_2 values increased slightly during the hypercapnia going on average from 106.04 ± 1.12 mm Hg to 109.32 ± 1.10 mm Hg in the younger group and from 101.61 ± 0.99 mm Hg to 105.54 ± 0.94 mm Hg in the older group. The manipulation was tolerable for participants of both age groups, with discomfort ratings of 2.16 ± 0.17 and 2.26 ± 0.19 for the younger and older

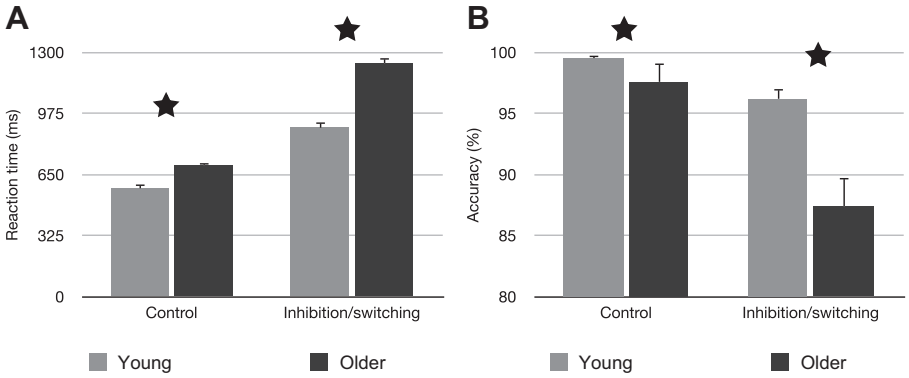

Fig. 2. Modified Stroop behavioral response. Reaction time in ms (A) and accuracy in percent correct responses (B) were both significantly different between the younger and older groups ($p < 0.0001$). The interaction between age group and block type (control or inhibition/switching) were also statistically significant ($p < 0.0001$ for reaction time and $p = 0.007$ for accuracy) and the cost of inhibition/switching was found to be higher in older than younger adults, indicating that the inhibition/switching is affected by age beyond the general effects of slowing and decreased accuracy seen in the control task (color naming). Statistical significance is indicated by a star.

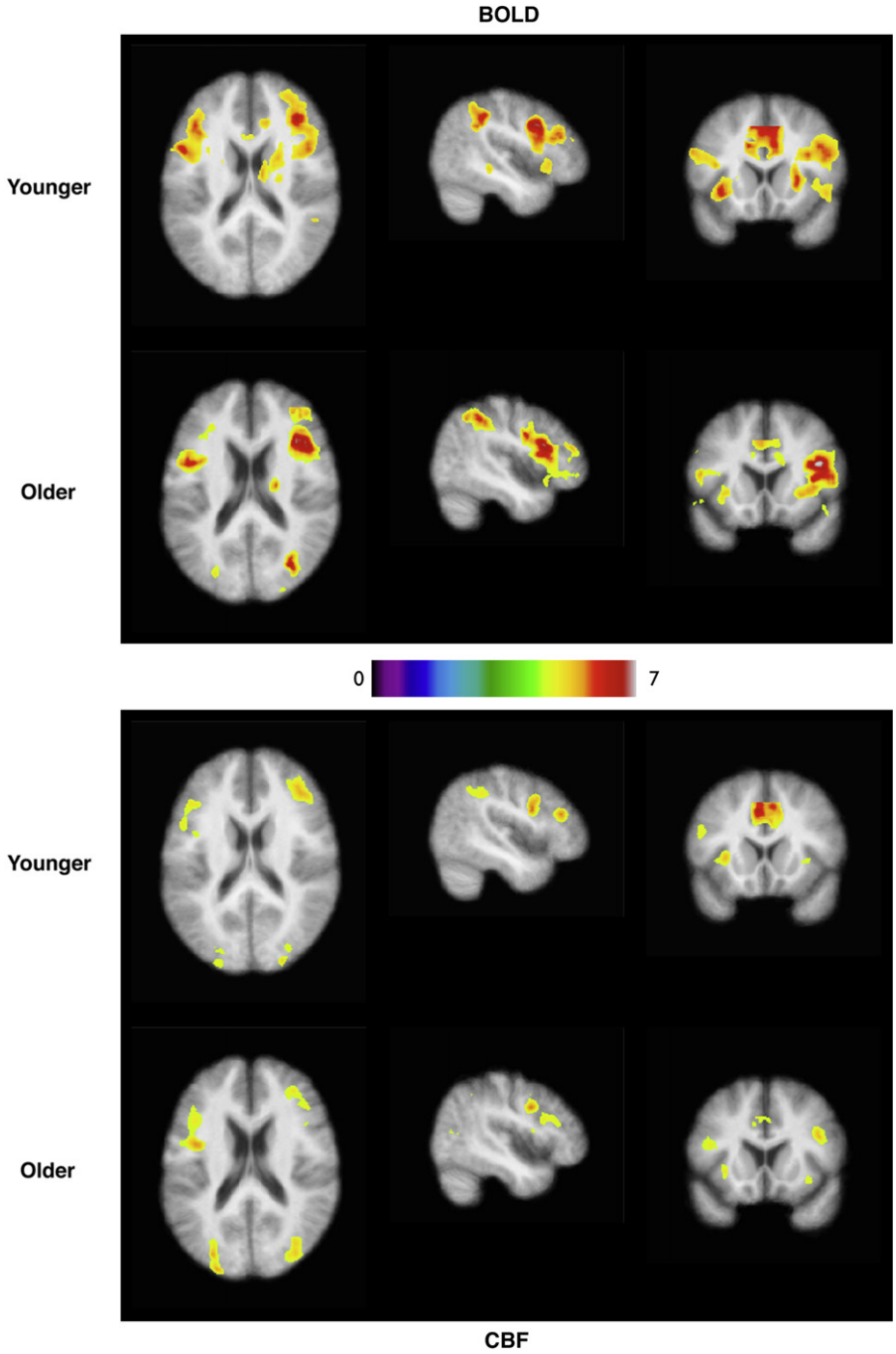

Fig. 3. Modified Stroop Z-score maps. Group activation maps for blood oxygen level-dependent (BOLD) and CBF in response to the Stroop task. These maps show the significant signal changes in response to the inhibition/switching blocks of the task. No significant difference was detected between maps from younger and older adults. Abbreviation: CBF, cerebral blood flow.

groups respectively on a possible range of 7 points (Banzett et al., 1996).

3.5. Vascular parameters

In contrast to the BOLD and CBF responses to the Stroop task, which were similar in both groups, other hemodynamic signals were found to be generally decreased in the older group. More specifically, BOLD responses to hypercapnia were found to be significantly lower in pooled ROIs ($p < 0.0001$) in the older group as compared with the young (Fig. 6 and Table 2). Individual ROIs were also associated with a significantly lower BOLD signal change in the older adults. Responses to the hypercapnia challenge were quantified over the 3 Stroop ROIs, and in complete gray matter. Average BOLD signal changes to CO_2 in gray matter were found to be 1.48 $\pm$ 0.07% and 1.01 $\pm$ 0.06% for younger and older adults respectively ($p < 0.0001$). All individual ROI average values are shown in Table 2.

Blood flow responses showed the same trend and average CBF responses in units of mL/100 g/min were generally lower in the older group and the main effect of age over all ROIs was found to be significant ($p < 0.0001$) (Fig. 7). Individual ROI averages can be

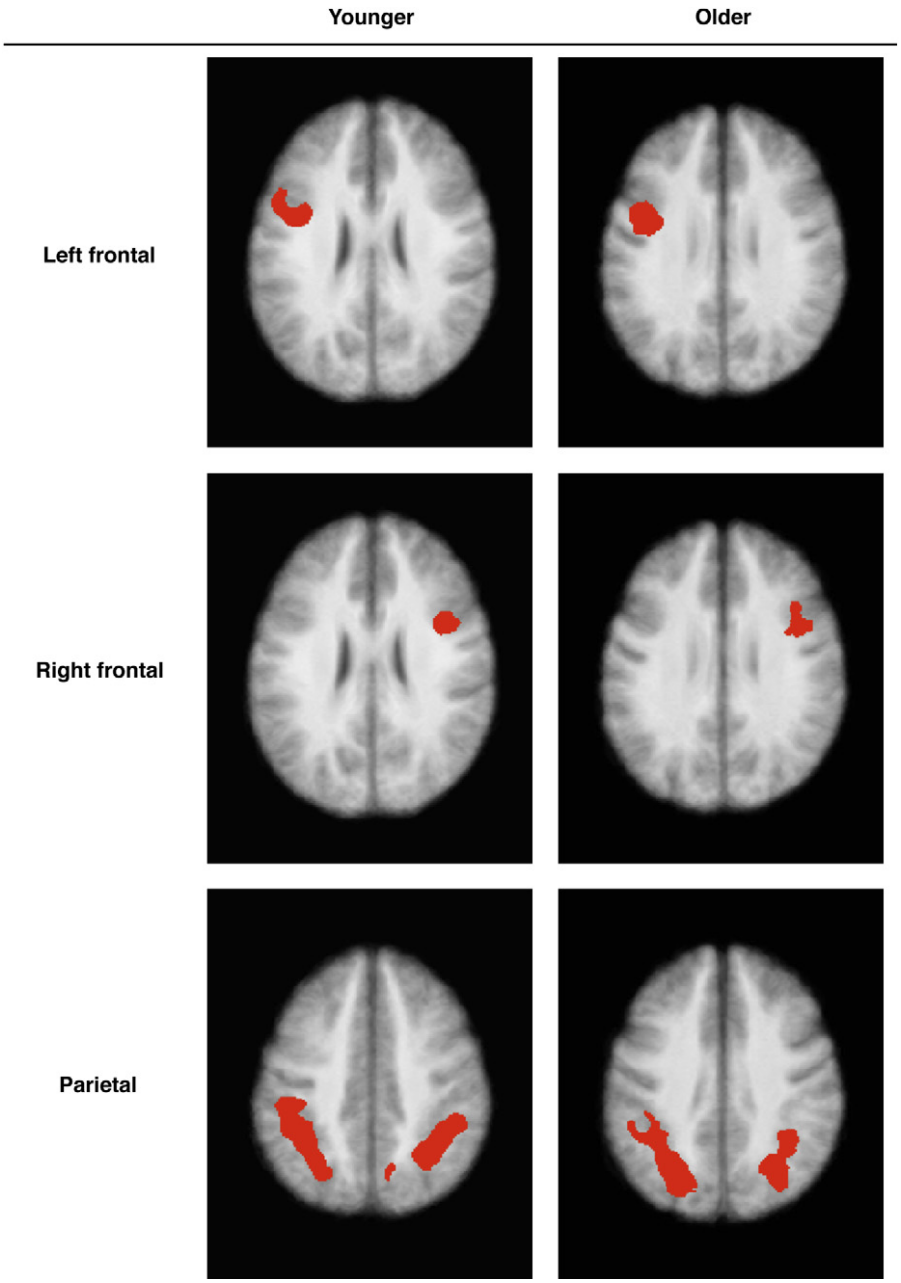

Fig. 4. Modified Stroop task regions of interest (ROIs). Group activation maps for the modified Stroop task yielded three main foci of cortical significant signal changes. These were used to delineate three ROIs in left frontal, right frontal, and parietal cortex. Signal changes and other physiological estimates were quantified within these ROIs for each participant.

found in Table 2. CBF changes over gray matter were found to be significantly lower in the older group, with values of 14.32 ± 1.01 mL/100 g/min in the younger and 10.00 ± 1.24 mL/100 g/min in the older group ($p < 0.01$). Left frontal estimates were on the other hand similar between the 2 groups ($p = 0.13$), and right frontal estimates showed the largest difference between groups ($p < 0.0002$). Finally, results in the parietal ROI showed a trend toward lower values in the older group ($p = 0.02$). Though flow changes in terms of absolute flow represent a more physiologically meaningful quantity, these changes are often reported as percentages in the extant literature. To facilitate comparisons with previous literature and because percent change values in CBF are used as input in the calibrated fMRI model, these values are reported in Table 2.

Percent BOLD and CBF changes during hypercapnia can also be converted to cerebrovascular reactivity (CVR) by dividing the percent change in CBF or BOLD by the change in end-tidal PCO_2 (Forbes et al., 1997; Gauthier et al., 2012; Graham et al., 1994; Mandell et al., 2008). CVR is likely to be a factor in determining the amplitude of task-induced changes in BOLD and CBF, because it quantifies the increase in signal per unit of vasodilatory signal. Because end-tidal PCO_2 increases were similar between the two groups, CVR values follow the same trend as percent changes. BOLD CVR was found to be significantly lower in the older group in pooled ROIs ($p < 0.0001$), with values of 0.31 ± 0.06 %ΔBOLD/mm Hg in the younger group and 0.23 ± 0.01 %ΔBOLD/mm Hg in the older group over gray matter. BOLD CVR was also significantly lower in all other individual ROIs ($p < 0.003$ in all cases), as shown in Fig. 8B and Table 2.

CBF vascular reactivity was more similar between the two groups than BOLD reactivity measured, though generally also significantly

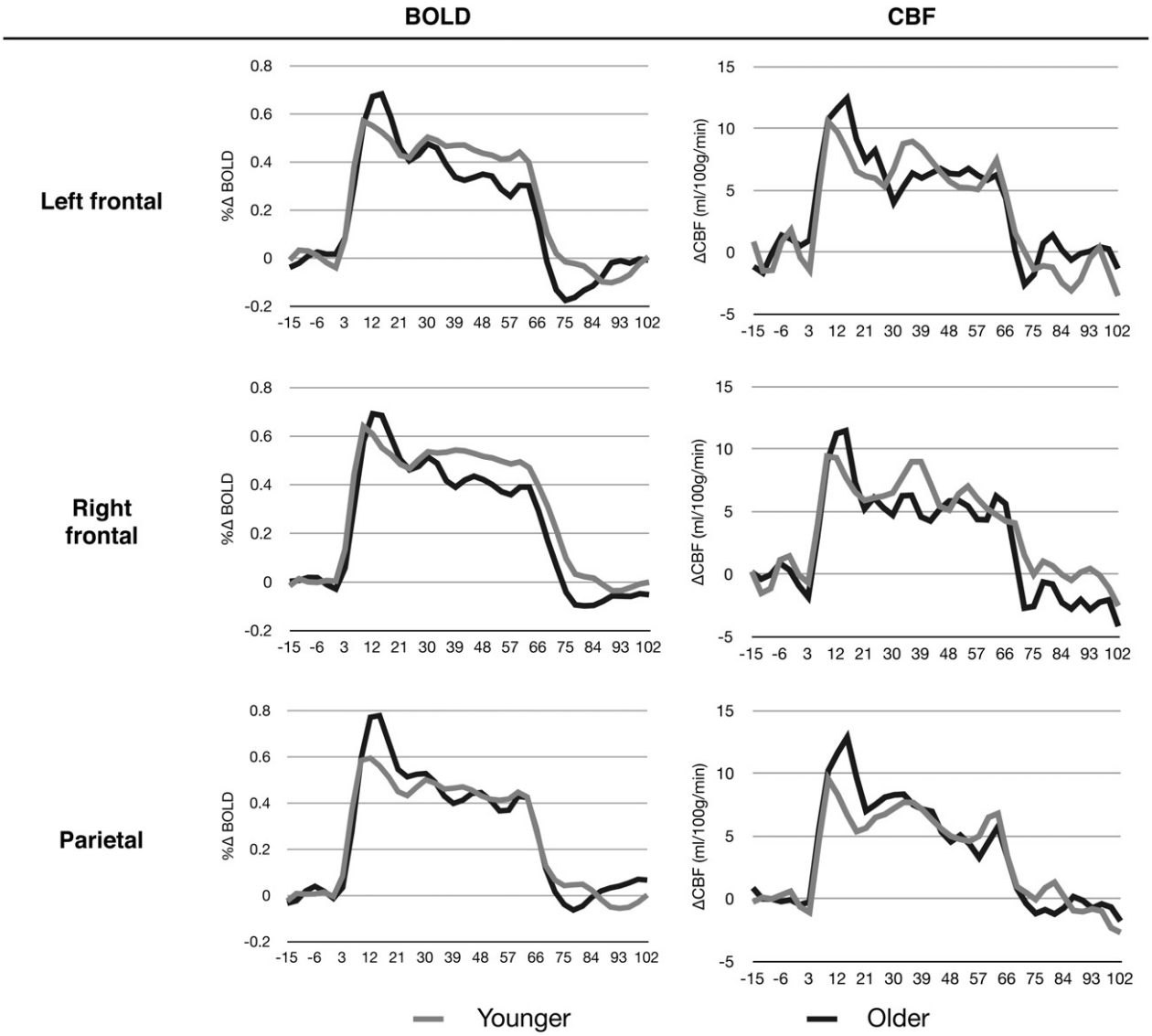

Fig. 5. Percent blood oxygen level-dependent (BOLD) and cerebral blood flow (CBF) responses to the modified Stroop task. Time courses showing BOLD and CBF responses to the modified Stroop task over the three functionally-defined regions of interest (ROIs): left frontal, right frontal, and parietal areas. Similar BOLD and CBF changes were observed in younger and older adults over all ROIs.

lower over all ROIs in the older group ($p < 0.0001$) (Fig. 8C and Table 2 for individual ROI quantifications). Gray matter and right frontal CVR were found to be significantly lower in the older group ($p < 0.004$), with values of 3.00 ± 0.18 (mL/100 g/min)/mm Hg in the younger and 2.14 ± 0.22 (mL/100 g/min)/mm Hg in the older group over gray matter. The left frontal estimates were similar between the two groups however ($p = 0.26$), and parietal estimates showed a trend toward lower values in the older participants ($p = 0.04$). CVR is often expressed as percentage CBF change in the literature and, to facilitate comparison with other studies, these values expressed as percentages are included in Table 2.

Baseline CBF was also found to be significantly lower across all ROIs in the older group as compared with the younger ($p < 0.0001$) (Fig. 8A and Table 2). Average gray matter baseline CBF was 57.94 ± 2.51 mL/100 g/min in younger and 50.20 ± 1.90 mL/100 g/min in the older group. Individual ROI averages are shown in Table 2 and these generally show a trend toward lower values in the older group, with p values slightly above the multiple comparison threshold (p values between 0.02 and 0.05, with threshold for multiple comparisons at $p = 0.013$).

3.6. Calibrated fMRI estimates

BOLD and CBF percent changes in response to CO_2 can be combined to estimate the maximum possible BOLD signal change, also called M in the calibrated fMRI literature. The calibration parameter M was quantified in individual subjects and ROIs (Fig. 9A and Table 2). Values pooled over all ROIs showed a significant decrease in M values in the older group ($p = 0.003$). In individual ROIs, the average values in the older group were generally lower than in the younger, and a tendency toward significance was identified in gray matter, with values of $5.72 \pm 0.22\%$ and $5.00 \pm 0.30\%$ for younger and older participants respectively ($p = 0.05$). Parietal estimates in the older group were found to be significantly lower than in the younger group ($p = 0.003$). Frontal estimates did not differ significantly between the two groups ($p \geq 0.09$).

Task-evoked $CMRO_2$ in each ROI was determined using group average values for all input parameters to benefit from additional averaging. Evoked $CMRO_2$ estimates during the modified Stroop task over individual ROIs can be found in Fig. 9B and Table 2. These estimates are associated with high variance because they are derived

Table 2
ROI quantification results

	Younger				Older			
	Left frontal	Right frontal	Parietal	Gray matter	Left frontal	Right frontal	Parietal	Gray matter
Stroop								
%Δ BOLD	0.50 ± 0.04	0.50 ± 0.04	0.47 ± 0.04		0.48 ± 0.03	0.50 ± 0.05	0.49 ± 0.04	
Δ CBF mL/100 g/min	6.54 ± 0.80	5.59 ± 0.86	5.83 ± 0.52		6.87 ± 0.78	7.17 ± 0.88[a]	7.65 ± 0.70[b]	
%Δ CBF	11.92 ± 1.73	9.47 ± 1.70	12.18 ± 1.40		13.80 ± 1.53	14.21 ± 1.52	17.56 ± 1.44	
%Δ $CMRO_2$	3.20 ± 1.54	1.07 ± 1.46	3.04 ± 1.23		3.25 ± 1.48	4.57 ± 1.58	4.04 ± 1.43	
Hypercapnia								
%Δ BOLD	1.11 ± 0.07	1.21 ± 0.07	1.37 ± 0.07	1.48 ± 0.07	0.81 ± 0.05[a]	0.86 ± 0.06[c]	0.87 ± 0.06[c]	1.01 ± 0.06[c]
Δ CBF ml/100 g/min	12.54 ± 1.20	15.50 ± 1.06	15.77 ± 0.95	10.00 ± 1.24	10.09 ± 21.08	9.59 ± 1.03[c]	12.04 ± 1.24[b]	14.32 ± 1.01[a]
%Δ CBF	22.16 ± 2.17	26.56 ± 2.08	32.78 ± 2.67	24.92 ± 1.37	21.62 ± 2.60	19.55 ± 1.96	30.55 ± 3.52	20.67 ± 2.58
%Δ BOLD/mm Hg	0.24 ± 0.02	0.26 ± 0.02	0.29 ± 0.02	0.31 ± 0.06	0.18 ± 0.01[a]	0.20 ± 0.01[a]	0.20 ± 0.01[c]	0.23 ± 0.01[c]
Δ CBF mL/100 g/min/mm Hg	2.62 ± 0.22	3.25 ± 0.20	3.33 ± 0.18	3.00 ± 0.18	2.25 ± 0.22	2.22 ± 0.26[a]	2.71 ± 0.23[b]	2.14 ± 0.22[a]
Baseline								
CBF mL/100 g/min	59.46 ± 2.85	60.87 ± 2.77	52.86 ± 3.09	57.94 ± 2.51	50.07 ± 2.58[b]	52.12 ± 2.76[b]	44.39 ± 2.74[b]	50.20 ± 1.90[b]
M%	5.24 ± 0.48	4.78 ± 0.31	4.67 ± 0.03	5.72 ± 0.22	4.78 ± 0.31	4.33 ± 0.36	3.41 ± 0.27[a]	5.00 ± 0.30[b]
SNR								
BOLD	276.71 ± 10.69	281.86 ± 11.14	278.44 ± 8.47	225.55 ± 7.71	265.87 ± 11.30	280.69 ± 12.28	290.18 ± 11.06	205.35 ± 9.25
ASL	3.33 ± 0.13	3.81 ± 0.15	3.63 ± 0.13	2.80 ± 0.13	2.63 ± 0.12[c]	2.84 ± 0.13[c]	2.85 ± 0.12[c]	1.81 ± 0.13[c]

This table compiles all the group average region of interest (ROI) results. Blood oxygen level-dependent (BOLD) responses to the Stroop and hypercapnia are expressed as percent changes, cerebral blood flow (CBF) responses to the Stroop and hypercapnia challenges are expressed in mL/100 g/min and percent change, evoked cerebral metabolic rate of O_2 consumption ($CMRO_2$) is expressed in percent change, baseline CBF in mL/100 g/min and the *M* value represents a percent. Temporal signal-to-noise ratio (SNR) values are also shown for each ROI. Stroop responses were only quantified in the three functionally-defined ROIs (left frontal, right frontal, and parietal), and responses to the hypercapnia challenge and baseline properties were additionally quantified in complete gray matter. An α level equivalent to 0.013 is used to assess significance when correcting for multiple comparisons across all measures (CBF changes were only compared between groups in mL/100 g/min).

[a] $p < 0.01$.
[b] $p < 0.05$.
[c] $p < 0.001$.

from a combination of three noisy measurements (percent BOLD and CBF evoked by the task and *M*) and no significant age effect was found across ROIs.

3.7. tSNR

tSNR of BOLD and CBF was quantified using the Stroop time series. This quantity represents the average baseline term over each time series, divided by the residuals from the GLM fit, averaged over all participants within each group. tSNR is a measure of the signal to noise ratio associated with temporal fluctuations in the signal, arising from a combination of instrumental thermal noise and fluctuations from physiological sources (e.g., cardiac and respiratory). As can be qualitatively ascertained in the maps shown in Fig. 9A, tSNR of the ASL data was lower in the older group as compared with the younger. This decrease seems especially

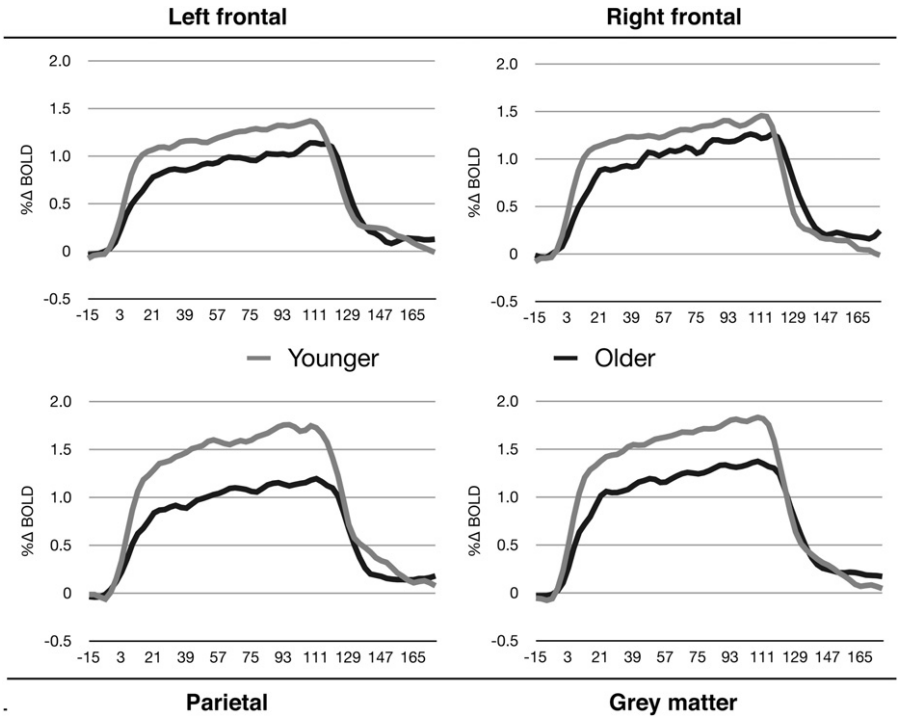

Fig. 6. Blood oxygen level-dependent (BOLD) hypercapnia time courses. Time courses of BOLD signal change in response to hypercapnia over all functionally determined regions of interest (ROIs) (left frontal, right frontal, parietal) and over all gray matter. BOLD responses to hypercapnia were lower in all ROIs in the older group ($p < 0.0001$).

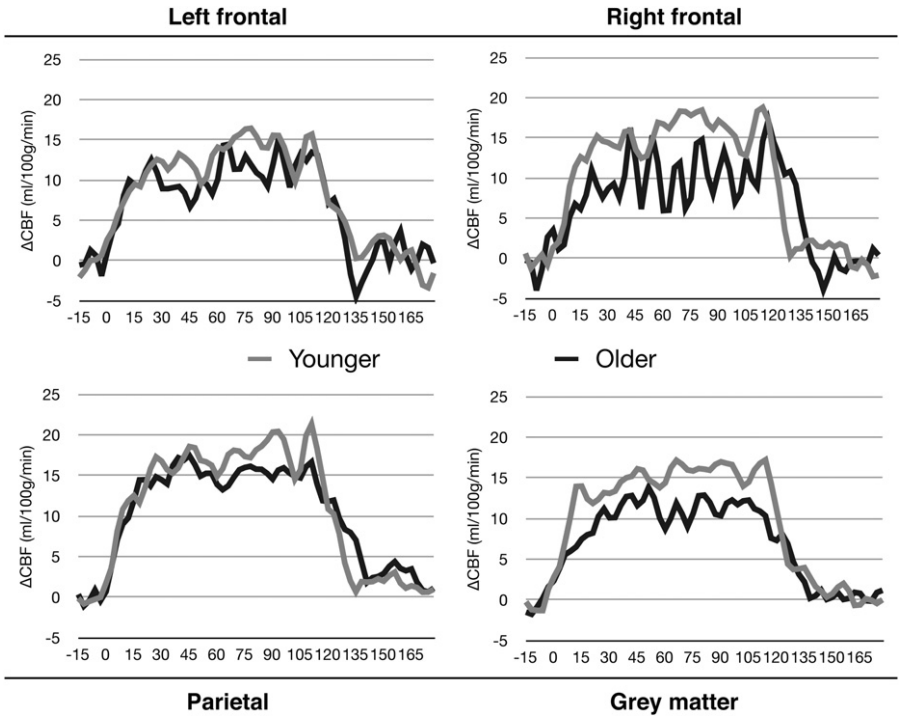

Fig. 7. Cerebral blood flow (CBF) hypercapnia time courses. Time courses of CBF change with hypercapnia, in absolute units of mL/100 g/min over all functionally determined regions of interest (ROIs) (left frontal, right frontal, parietal) and over all gray matter. Though an overall effect of age was found and CBF response to hypercapnia was found to be generally lower in the older group ($p < 0.003$), individual ROIs did not show a significant difference.

pronounced in more frontal areas. BOLD tSNR however, was similar between the two groups (Fig. 10A). Quantifications within the different ROIs confirmed that tSNR was significantly lower in all ROIs used in this study for ASL ($p < 0.0001$) (Fig. 10B and Table 2), but no significant difference was identified for BOLD data ($p = 0.48$) (Fig. 10C and Table 2). BOLD tSNR values were 225.55 ± 7.71 and 205.35 ± 9.25 in gray matter for young and older respectively. ASL tSNR was generally fairly low and even lower across all ROIs in the older group ($p < 0.0001$), with values of 2.80 ± 0.13 and 1.81 ± 0.13 in the younger and older group respectively in the gray matter ROI ($p < 0.0001$). All ROI average values can be found in Table 2.

4. Discussion

Neuroimaging studies of cognition typically use the BOLD signal to localize brain regions involved in the performance of a task. Cognitive studies of aging often compare the BOLD signal changes in groups of young and older adults in the context of tasks known to be associated with significant behavioral age-related differences. The assumption made in such studies is that the BOLD signal can be taken as a direct index of neuronal activity. However, there is reason to believe that this simplifying assumption might not be valid when comparing groups of widely different ages, because significant vascular changes are known to occur during adult life (Chen et al., 2011; Lu et al., 2011; O'Rourke and Hashimoto, 2007; Samanez-Larkin and D'Esposito, 2008). The results of the present study indicate that caution must be exercised when making these direct comparisons and that there are in fact profound vascular biases associated with age. Age-related vascular changes might mask some metabolic differences and lead to erroneous conclusions when only BOLD results are taken into account to make inferences about the neuronal resources used during performance of a task.

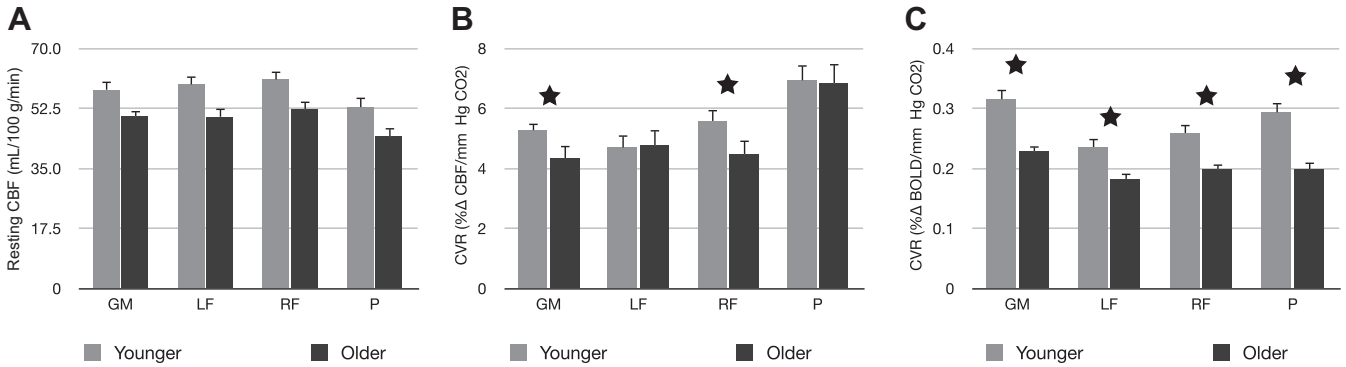

Fig. 8. Baseline cerebral blood flow (CBF) and cerebrovascular reactivity (CVR). This figure shows baseline CBF values in units of mL/100 g/min (A), CBF CVR in units of percent CBF change per mm Hg end-tidal partial pressure of CO_2 (PCO_2) increase (B), and blood oxygen level-dependent (BOLD) CVR in units of percent BOLD signal change per mm Hg end-tidal PCO_2 increase (C) for all regions of interest (ROIs). Baseline CBF showed a trend toward a lower baseline flow in the older group over pooled ROIs ($p < 0.0001$), and only BOLD CVR differed significantly over all ROIs ($p < 0.002$). Significance at the individual ROI level is indicated by a star. Abbreviations: GM, gray matter; LF, left frontal; P, parietal; RF, right frontal.

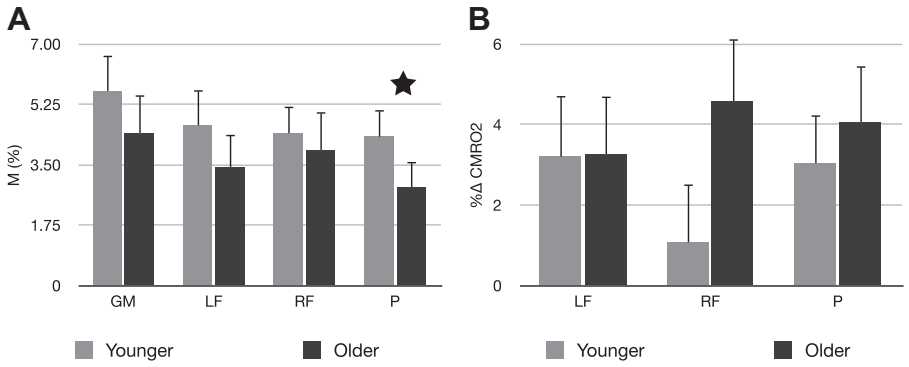

Fig. 9. *M* and cerebral metabolic rate of O_2 consumption ($CMRO_2$) values. This figure compares the calibrated functional magnetic resonance imaging parameters *M* (A) and percent evoked $CMRO_2$ to the modified Stroop task (B) between the younger and older groups. $CMRO_2$ was only quantified in the functionally-determined regions of interest (ROIs), and *M* was quantified over an additional gray matter (GM) ROI because it is not a task-based measurement. Values of *M* were found to be generally lower in the older group ($p = 0.0002$ for pooled ROIs). Similar $CMRO_2$ estimates might reflect the fact that variance on this estimate is high because it is a composite estimate from four measurements. Significance at the individual ROI level is indicated by a star. Abbreviations: LF, left frontal; P, parietal; RF, right frontal.

4.1. BOLD measurement of the cognitive task

The results presented here go beyond the standard sets of measures usually collected in the context of a cognitive imaging study of aging, but do in fact include them. If one were to look simply at the BOLD data evoked by the modified Stroop task collected here (Figs. 3 and 5), one would draw the conclusion that older adults use neuronal resources to perform this task similar to younger individuals, but that this similarity stands in contrast to the widely differing behavioral responses (Fig. 2). The lower behavioral performance of older adults in the context of similar brain responses could be suggestive of a ceiling effect, possibly because of brain atrophy in older adults (Reuter-Lorenz and Cappell, 2008; Schneider-Garces et al., 2010). This task is fairly difficult, because

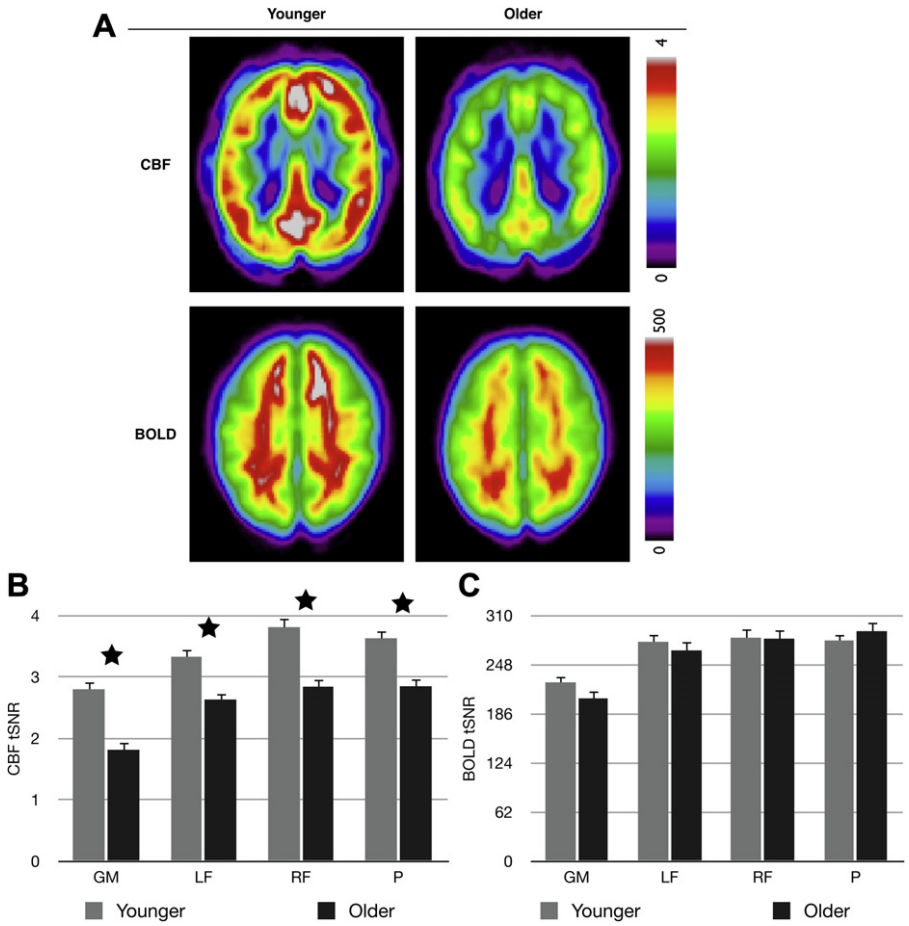

Fig. 10. Temporal signal-to-noise ratio (tSNR) of cerebral blood flow (CBF) and blood oxygen level-dependent (BOLD) measurements. tSNR maps of ASL and BOLD (A) show a decrease in ASL tSNR over all gray matter in the older group, with some spatial heterogeneity. Quantification of tSNR in functionally-defined and gray matter regions of interest (ROIs) show that ASL tSNR (A) was significantly lower in all ROIs ($p < 0.0001$), and BOLD tSNR (B) was found to be fairly stable across age. Significance at the individual ROI level is indicated by a star.

a set of two rules and two possible answers must be kept in mind at all times, and any set of rules and answers might be required at any time during the inhibition/switching blocks. It could therefore be that the older adults have reached their own maximal usage of neuronal resources and that they in fact perform more poorly on the task because they could not recruit the additional resources they needed to match the performance of younger adults (Park and Reuter-Lorenz, 2009; Reuter-Lorenz and Park, 2010). One could speculate this to be because of atrophy or other changes such as decreased perceptual acuity and dedifferentiation from changes in the neuromodulatory system (Baltes and Lindenberger, 1997; Li and Sikstrom, 2002; Park and Reuter-Lorenz, 2009).

The results obtained from a BOLD-only acquisition of a cognitive task do not however allow us to answer these questions, because of the physiological ambiguity of the BOLD signal. Though studies have shown that the amplitude and shape of the BOLD response is related to synaptic activity in individual primate subjects (Logothetis et al., 2001; Shmuel et al., 2002), the relationship between synaptic activity measured using local field potential electrophysiology and BOLD signal amplitude and shape is complex and nonlinear (Magri et al., 2012). Neuronal activity leads to the release of a variety of vasoactive signals (Girouard and Iadecola, 2006; Lecrux and Hamel, 2011) that determine the characteristics of the hemodynamic response measured using the BOLD contrast. Though the main mediators of neurovascular coupling are fairly well established, the quantitative relationship between these molecules and the blood flow and volume increase is unknown (Girouard and Iadecola, 2006; Lecrux and Hamel, 2011). Furthermore, we do not as yet know how all these mechanisms are affected by aging. More specific vascular and metabolic information is needed to better interpret the observed BOLD responses in terms of neuronal activity, because BOLD alone cannot be readily converted into a quantitative measure of synaptic activity and because the factors that determine this relationship are likely to be affected by age.

4.2. Blood flow measurements during the cognitive task

Though these questions cannot all be answered with the present dataset, the additional information provided does improve our understanding of the physiological events. One pertinent piece of information is provided by blood flow changes during the task. ASL techniques allow the measurement of changes in CBF (Williams et al., 1992), which represents a more physiologically specific quantity and can inform us on one of the factors contributing to the BOLD signal. Here we can see that the CBF change evoked by the task was in most ROIs, as seen for BOLD, similar between the two groups in terms of amplitude and shape (Figs. 3 and 5). Therefore, this measurement also leads us to believe that similar neural resources are used by younger and older adults for the performance of this task. A modest trend towards higher CBF increases in all ROIs and a statistically significant difference in the right frontal ROI indicate, however, that there might be a tendency for older individuals to have a larger increase in metabolism and hence, presumably, in neuronal activity during the task. This higher response might furthermore be highest in some regions, which agrees well with previous literature on lateralization changes in cognitive studies of aging (Cabeza, 2002; Cappell et al., 2010; Park and Reuter-Lorenz, 2009; Reuter-Lorenz and Park, 2010; Schneider-Garces et al., 2010).

4.3. Hypercapnic responses

It might, however, be that similar signal changes in younger and older adults reflect different metabolic expenditures if the hemodynamic properties of older brains are changed because of vascular impairments. Aging has been shown to be associated with vascular impairments such as arterial hardening from increased collagen content of arterial walls and decreased vascular density (Brown and Thore, 2011; O'Rourke and Hashimoto, 2007; Sonntag et al., 1997). Because these have the potential to profoundly affect CBF, they could also affect the BOLD signal amplitude measured in response to the task. The clearest indication that this might be the case is that the BOLD response to a hypercapnia challenge was found to be significantly reduced in the older adults. CO_2 has vasodilatory properties and its inhalation triggers an increase in blood flow throughout gray matter. Furthermore, previous studies have shown that this increase in blood flow, and hence in BOLD signal, is linearly proportional to the concentration of CO_2 in the inspired air, when CO_2 is given as here in small concentrations (Hoge et al., 1999b; Mark et al., 2010; Stefanovic et al., 2006). The reduced BOLD responses to hypercapnia in older adults confirm the capability of BOLD to capture age-related physiological differences in the brain regions probed in the present study. It also indicates that there are some underlying hemodynamic changes in the elderly, not visible from BOLD measurements of task alone. A reduced reactivity to CO_2 could indicate that the coupling of vasodilatory signal to flow increase is degraded in older subjects. This could be because of vessel hardening, especially because the brain is known to be one of the only organs in the body without protection against the pulsatile effects of flow, and might hence be more sensitive to long-term damage (O'Rourke and Hashimoto, 2007). However, because the BOLD signal is intrinsically ambiguous and arises from a combination of sources, we cannot know from this alone which components of the response is affected by aging.

Once again, we can turn to the ASL data to get a more physiologically specific measurement. An additional advantage of ASL over BOLD measurements is that resting blood flow in absolute units of mL/100 g/min can readily be obtained. This is not only an important parameter of itself, but can also be used to convert percent changes into flow change in absolute units. This allows quantitative comparisons between groups, such as in younger and older adults, known to exhibit differences in baseline flow (Chen et al., 2011). Both baseline blood flow and absolute changes in response to hypercapnia were found to be lower in older adults across pooled ROIs. This might be indicative of a lower vascular tone in the older adults, possibly because of damage to blood vessel walls from the pulsatile effect of blood (O'Rourke and Hashimoto, 2007). This finding is furthermore in agreement with previous literature also showing age-related decreases in flow CVR (Ances et al., 2009; Lu et al., 2011).

4.4. Calibrated fMRI measurements

Taken together, CBF and BOLD response to hypercapnia can be used to calculate the BOLD calibration factor *M*. This corresponds to the BOLD signal attenuation at rest, attributable to the baseline deoxyhemoglobin (dHb) brain content. Because this is calculated using a ratio of BOLD and CBF, this measurement suffers from having a low SNR. Values of *M* were found to be significantly lower in the older group than in the younger group for pooled ROI values. A similar trend toward lower *M* values in older adults has been observed in other calibrated fMRI studies of aging (Ances et al., 2009; Mohtasib et al., 2012). This means that in the older group, the amplitude scaling of BOLD for a given fractional change in dHb is reduced because of a lower initial dHb content of venous blood. Because blood flow increases more than metabolism after neuronal activity (Buxton, 2010; Hoge et al., 1999a), it is in part the dHb concentration present at rest that determines how much the BOLD signal can increase during performance of a task (because baseline

dHb is one of the sources of decreased BOLD signal that is diluted by activity-dependent flow increases). Because the BOLD amplitude scaling is reduced, it might therefore be that a larger amount of oxidative metabolism is needed to evoke a similar CBF and BOLD response.

The measurement of BOLD and CBF responses to the task, combined with the *M* parameter estimated before, can be used to estimate the fractional change in $CMRO_2$ evoked by the task. This parameter represents a more specific physiological property than the BOLD signal, and might be compared between groups. Furthermore, because the greater part of the metabolism evoked after neuronal activity is thought to be oxidative (Hattori et al., 2004; Ibaraki et al., 2008, 2010; Ishii et al., 1996; Ito et al., 2005; Mintun et al., 2002; Yamauchi et al., 2002), it is also a quantity more directly related to neuronal function than BOLD signal or measurements of CBF. The precision of this estimate is unfortunately limited, because it is computed as a function of four low SNR measures. Although no significant differences were thus detected in this group, the differences in BOLD and CBF responses to CO_2 were consistent with a trend toward an increase in $CMRO_2$ in the older group in response to the task, despite the similarity in the measured responses to the task.

4.5. Potential confounds

In this study, we sought to isolate the effects of age and selected our older cohort using very strict selection criteria to exclude older adults with vascular risk factors such as high blood pressure (including medically controlled blood pressure), hypercholesterolemia, and smoking. However, the Canadian Health Measure Survey indicates that adults in the age range included in this study (55–75 years) might be at a vulnerable time of life for developing heart conditions. Within this age range the incidence of high blood pressure increases very steeply from 18.4% in the 40–69-year-old population to 53.2% observed for the next two decades. Adults included in this study were also highly educated, with an average number of years of education at 16.3 ± 3.4, corresponding to 5 years of postsecondary education in the province of Quebec. This is greater than the national average of 13.2 years for adults between the ages of 25 and 54 years reported from the 1996 Canadian census. Therefore, the results of this study likely represent an underestimation of the effects observable in the general aging population, because these individuals are in better health and more educated than the general population within the same age range. If the effects of age on BOLD signal properties are expected to stem from deteriorating vascular health, then the healthier the arteries, the smaller the effects of age will be. In this case, because our exclusion criteria ensured that none of our participants had the usual hallmarks of poor vascular health, such as high blood pressure, high blood cholesterol, and fasting glucose levels, we expect these older adults to be much more similar in terms of vascular health to young participants than less healthy older adults.

The relatively small amplitude of difference between the two groups might also be attributable to several other factors. The sample sizes used here, though larger than those used in most other calibrated fMRI studies, might still be too small to detect the small differences present in a group of very healthy older adults, particularly when only a single scanning run of the modified Stroop task was performed. In typical cognitive fMRI studies, several repetitions of the task are usually performed to maximize statistical power. However, time constraints in this comprehensive imaging protocol, which also included a thoracic MRI exam to be discussed in a separate publication, precluded the acquisition of additional modified Stroop runs. Finally, baseline $CMRO_2$ might be different in the two groups. There is some indication that baseline $CMRO_2$ might be changed in older adults, though the existing literature does not agree on the direction of the change, with positron emission tomography results showing a decrease with age (Leenders et al., 1990; Marchal et al., 1992; Yamaguchi et al., 1986) and results from a recent MRI study showing an increase (Lu et al., 2011). Therefore, even if equivalent fractional changes in $CMRO_2$ are estimated, it might be that there is in fact a difference in evoked $CMRO_2$ in absolute units between the two groups, when expressed in terms of micromolar O_2 usage for a given tissue volume. Though we cannot determine here if this is the case, future studies using a method recently developed in our group will address this issue (Gauthier and Hoge, 2012b).

Another parameter that was noted to be significantly different in the two age groups was the tSNR of ASL as illustrated in Fig. 10B. tSNR takes into account the temporal fluctuations in time series. These fluctuations are thought to be a combination of instrumental thermal noise and fluctuations from physiological sources such as heart beats and respiration changes (Kruger and Glover, 2001; Triantafyllou et al., 2005). This difference in ASL tSNR can be contrasted to the BOLD tSNR in gray matter, which was much more comparable between the two groups and for which the difference did not attain statistical significance (Fig. 10C). As the variance of BOLD signals in gray matter is believed to be dominated by physiological noise under the conditions of our study (3 Tesla, large voxels), it would appear that the age-related differences ASL tSNR might be because of physical noise sources that affect the actual MRI signal strength and instrumentation noise. This is also supported by the observation that BOLD tSNR in the young group was substantially higher in white matter (Fig. 10A), in which instrumental noise is likely to be more predominant. Higher instrumental noise in older subjects could be associated with differences in coil loading or shimming associated with systematic postural and anatomical differences that were noted (e.g., kiphotic spine, higher body fat). Alternatively, the lower ASL tSNR could reflect an increased variability in the ASL labeling signal, in addition to a reduction in its mean amplitude. Such an increase in variability might be because of differences in heart rate and blood flow velocity in the two groups, or other physiological factors. The effect of age on ASL labeling parameters for pseudocontinuous ASL sequences are unknown, but reduced labeling efficiency has been previously demonstrated for pulsed ASL sequences (Campbell and Beaulieu, 2006). This means that age-dependent comparisons of neuronal activation based solely on the spatial extent of significant ASL response in a functional study must be treated with caution because this metric might be biased by the different tSNR levels.

4.6. Limitations

The sample size and limited data averaging possible in this study did not permit the investigation of the difference contrast between the inhibition/switching and control components of the task. Though this does not prevent asking questions about the physiologic properties of the areas of the brain involved in the task, it allows only a limited discussion of their implications in the context of cognitive aging. Furthermore, it might be that the task used in this study was not optimal for finding differences between young and old adults. The task used here was chosen to maximize age-related differences in behavioral response. Though the Stroop task is frequently used in studies of aging, some studies have suggested that tasks including an element of switching might be more vulnerable than interference to the effects of aging (Wasylyshyn et al., 2011). This task was therefore chosen because it is well characterized and expected to show large performance changes with aging (Bohnen et al., 1992; Gauthier et al., 2012). However, though age is associated with large changes in performance on

these types of tasks, the fMRI results are less clear. Tasks with a switching component, such as the modified Stroop task used here, are expected to yield bilateral prefrontal activation, because these areas are involved both in inhibition and task switching (DiGirolamo et al., 2001; Dove et al., 2000; Langenecker et al., 2004; Leung et al., 2000; MacDonald et al., 2000; Milham et al., 2002; Prakash et al., 2011; Yeung et al., 2006; Zysset et al., 2007). Studies of aging using the Stroop task have generally found an increased extent or amplitude of the hemodynamic response in the older group than in the younger group during inhibition (Langenecker et al., 2004; Prakash et al., 2011; Zysset et al., 2007), though at least one study found the opposite trend (Milham et al., 2002). There are few fMRI studies of switching tasks with aging, but one study (DiGirolamo et al., 2001) found that older and younger adults recruit similarly dorsolateral prefrontal cortex and medial frontal cortex areas. In the present study, we also found similar BOLD signal patterns during inhibition/switching blocks in both age groups. Another study of switching during aging found, however, older adults to show smaller BOLD signal changes in response to the task in frontal and parietal regions (Gold et al., 2010), which is not the pattern observed here. The task used in that study was however different and the group of participants smaller, with less stringent selection criteria, indicating a perhaps less healthy cohort.

Aging is associated with loss of tissue in the brain (Salat et al., 2004). Partial volume effects must therefore be taken into account when making age comparisons, especially when using functional techniques such as ASL which are limited in terms of spatial resolution. Comparisons made without taking these partial volume effects into account could lead to underestimation of the effects seen in older as compared with younger individuals because smaller volumes of tissue might contribute to the signal. Here, the quantitative results obtained from ROI averaging were weighted by each voxel's gray matter fraction. Because this fraction was determined on an individual level using the anatomic data obtained in each participant, this might not however be a significant source of confound in our results.

Different breathing manipulations might be used for calibrated fMRI and a common concern with hypercapnia is that it might lead to breathing discomfort in participants. Breathing discomfort was rated using the 7-point rating scale presented by Banzett et al. (1996) and average ratings were 2.16 $\pm$ 0.17 and 2.26 $\pm$ 0.19 in the younger and older groups, respectively. This corresponds to a rating between no discomfort and mild discomfort. Therefore, discomfort of the breathing manipulation is unlikely to have acted as a significant confound in our data.

Another subject of debate with hypercapnia is whether it causes any changes in oxidative metabolism when small doses are administered. Results from the literature are unclear, with some reports of increases in metabolism (Horvath et al., 1994; Jones et al., 2005), decreases (Xu et al., 2011b; Zappe et al., 2008), and no detectable change (Chen and Pike, 2010a; Hino et al., 2000; McPherson et al., 1991). Because the literature lacks consensus on this topic, we have elected to preserve the assumption of no evoked metabolism usual for this type of study. However, were a consensus to be reached or a way of measuring a potential change in metabolism arise, this could be taken into account in the modeling in future studies.

4.7. Future directions

The present study identifies potential sources of bias in BOLD studies of cognitive aging and suggests that simple BOLD signal comparisons might not fully reflect the metabolic response elicited by a task in older brains. Interpretation would be further aided if absolute measures of resting $CMRO_2$ were available in our subjects. Because the calibrated fMRI method used here yields a fractional change from an unknown and possibly population-dependent baseline, we cannot determine from this result if the oxidative metabolism in micromolar units is truly different between groups. We have recently reported a technique, dubbed QUO2, which allows determination of resting oxygen extraction fraction (OEF) and $CMRO_2$ using two breathing manipulations (Gauthier and Hoge, 2012b). Future studies using this or other related techniques (Bulte et al., 2012) will add much-needed information on the metabolic aspects of aging and the possible effect of these changes on hemodynamic imaging techniques.

4.8. Conclusion

The present study indicates that BOLD-only studies of cognitive aging might be subject to biases that lead to underestimation of the oxidative metabolism underlying the BOLD signal changes seen in the elderly. BOLD and CBF responses to a hypercapnia functional challenge indicate that the reactivity and range of these imaging contrasts in older adults, masking to some extent increases in oxidative metabolism. These results warrant greater caution in the interpretation of BOLD signal changes observed in different age groups and highlight the importance of ancillary measures such as baseline blood flow and CO_2 reactivity which provide important information for the understanding of age-related functional imaging changes.

Disclosure statement

All authors have no conflict of interest to declare.

All subjects gave informed consent and the project was approved by the Comité mixte d'éthique de la recherche du Regroupement Neuroimagerie/Québec.

Acknowledgements

The authors thank Carollyn Hurst and André Cyr for help with data acquisition, Christopher Steele for help with data analysis and presentation, Felipe Tancredi for helpful discussions on data analysis, and Jiongjiong Wang at UCLA, who provided the pseudo-continuous arterial spin-labeling sequence used. This work was supported by the Canadian Institutes for Health Research (MOP 84378, Banting and Best Scholarship held by CJG), the Canadian Foundation for Innovation (Leaders Opportunity Fund 17380), the Canadian National Sciences and Engineering Research Council (R0018142), and the Ministère du développement économique, de l'innovation et de l'exportation (PSR-SIIRI-239).

References

Ances, B.M., Liang, C.L., Leontiev, O., Perthen, J.E., Fleisher, A.S., Lansing, A.E., Buxton, R.B., 2009. Effects of aging on cerebral blood flow, oxygen metabolism, and blood oxygenation level dependent responses to visual stimulation. Hum. Brain Mapp. 30, 1120–1132.

Baltes, P.B., Lindenberger, U., 1997. Emergence of a powerful connection between sensory and cognitive functions across the adult life span: a new window to the study of cognitive aging? Psychol. Aging 12, 12–21.

Banzett, R.B., Lansing, R.W., Evans, K.C., Shea, S.A., 1996. Stimulus-response characteristics of CO2-induced air hunger in normal subjects. Respir. Physiol. 103, 19–31.

Beckmann, C.F., Jenkinson, M., Smith, S.M., 2003. General multilevel linear modeling for group analysis in FMRI. Neuroimage 20, 1052–1063.

Blockley, N.P., Griffeth, V.E., Buxton, R.B., 2012. A general analysis of calibrated BOLD methodology for measuring CMRO(2) responses: comparison of a new approach with existing methods. Neuroimage 60, 279–289.

Bohnen, N., Jolles, J., Twijnstra, A., 1992. Modification of the Stroop Color Word Test improves differentiation between patients with mild head injury and matched controls. Clinical Neuropsychologist 6, 178–184.

Brown, W.R., Thore, C.R., 2011. Review: cerebral microvascular pathology in ageing and neurodegeneration. Neuropathol. Appl. Neurobiol. 37, 56–74.

Bulte, D.P., Kelly, M., Germuska, M., Xie, J., Chappell, M.A., Okell, T.W., Bright, M.G., Jezzard, P., 2012. Quantitative measurement of cerebral physiology using respiratory-calibrated MRI. Neuroimage 60, 582–591.

Buxton, R.B., 2010. Interpreting oxygenation-based neuroimaging signals: the importance and the challenge of understanding brain oxygen metabolism. Front. Neuroenergetics 2, 8.

Cabeza, R., 2002. Hemispheric asymmetry reduction in older adults: the HAROLD model. Psychol. Aging 17, 85–100.

Cabeza, R., Nyberg, L., Park, D.C., 2005. Cognitive Neuroscience of Aging: Linking Cognitive and Cerebral Aging. Oxford University Press, Oxford.

Campbell, A.M., Beaulieu, C., 2006. Pulsed arterial spin labeling parameter optimization for an elderly population. J. Magn. Reson. Imaging 23, 398–403.

Cappell, K.A., Gmeindl, L., Reuter-Lorenz, P.A., 2010. Age differences in prefontal recruitment during verbal working memory maintenance depend on memory load. Cortex 46, 462–473.

Chen, J.J., Pike, G.B., 2010. Global cerebral oxidative metabolism during hypercapnia and hypocapnia in humans: implications for BOLD fMRI. J. Cereb. Blood Flow Metab. 30, 1094–1099.

Chen, J.J., Rosas, H.D., Salat, D.H., 2011. Age-associated reductions in cerebral blood flow are independent from regional atrophy. Neuroimage 55, 468–478.

Chiarelli, P.A., Bulte, D.P., Wise, R., Gallichan, D., Jezzard, P., 2007. A calibration method for quantitative BOLD fMRI based on hyperoxia. Neuroimage 37, 808–820.

Cox, R.W., Jesmanowicz, A., 1999. Real-time 3D image registration for functional MRI. Magn. Reson. Med. 42, 1014–1018.

Davis, S.W., Dennis, N.A., Daselaar, S.M., Fleck, M.S., Cabeza, R., 2008. Que PASA? The posterior-anterior shift in aging. Cereb. Cortex 18, 1201–1209.

Davis, T.L., Kwong, K.K., Weisskoff, R.M., Rosen, B.R., 1998. Calibrated functional MRI: mapping the dynamics of oxidative metabolism. Proc. Natl. Acad. Sci. U. S. A. 95, 1834–1839.

Delis, D.C., Kaplan, E., Kramer, J.H., 2001. Delis-Kaplan Executive Function System (D-KEFS). The Psychological Corporation, San Antonio, TX.

DiGirolamo, G.J., Kramer, A.F., Barad, V., Cepeda, N.J., Weissman, D.H., Milham, M.P., Wszalek, T.M., Cohen, N.J., Banich, M.T., Webb, A., Belopolsky, A.V., McAuley, E., 2001. General and task-specific frontal lobe recruitment in older adults during executive processes: a fMRI investigation of task-switching. Neuroreport 12, 2065–2071.

Dove, A., Pollmann, S., Schubert, T., Wiggins, C.J., von Cramon, D.Y., 2000. Prefrontal cortex activation in task switching: an event-related fMRI study. Brain Res. Cogn. Brain Res. 9, 103–109.

Folstein, M.F., Folstein, S.E., McHugh, P.R., 1975. "Mini-mental state". A practical method for grading the cognitive state of patients for the clinician. J. Psychiatr. Res. 12, 189–198.

Forbes, M.L., Hendrich, K.S., Kochanek, P.M., Williams, D.S., Schiding, J.K., Wisniewski, S.R., Kelsey, S.F., DeKosky, S.T., Graham, S.H., Marion, D.W., Ho, C., 1997. Assessment of cerebral blood flow and CO2 reactivity after controlled cortical impact by perfusion magnetic resonance imaging using arterial spin-labeling in rats. J. Cereb. Blood Flow Metab. 17, 865–874.

Gauthier, C.J., Desjardins-Crépeau, L., Madjar, C., Bherer, L., Hoge, R.D., 2012. Absolute quantification of resting oxygen metabolism and metabolic reactivity during functional activation using QUO2 MRI. Neuroimage 63, 1353–1363.

Gauthier, C.J., Hoge, R.D., 2012a. A generalized procedure for calibrated MRI incorporating hyperoxia and hypercapnia. Hum. Brain Mapp. http://dx.doi.org/10.1002/hbm.21495.

Gauthier, C.J., Hoge, R.D., 2012b. Magnetic resonance imaging of resting OEF and CMRO2 using a generalized calibration model for hypercapnia and hyperoxia. Neuroimage 60, 1212–1225.

Gauthier, C.J., Madjar, C., Tancredi, F.B., Stefanovic, B., Hoge, R.D., 2011. Elimination of visually evoked BOLD responses during carbogen inhalation: implications for calibrated MRI. Neuroimage 54, 1001–1011.

Girouard, H., Iadecola, C., 2006. Neurovascular coupling in the normal brain and in hypertension, stroke, and Alzheimer disease. J. Appl. Physiol. 100, 328–335.

Glover, G.H., 1999. Deconvolution of impulse response in event-related BOLD fMRI. Neuroimage 9, 416–429.

Gold, B.T., Powell, D.K., Xuan, L., Jicha, G.A., Smith, C.D., 2010. Age-related slowing of task switching is associated with decreased integrity of frontoparietal white matter. Neurobiol. Aging 31, 512–522.

Goode, S.D., Krishan, S., Alexakis, C., Mahajan, R., Auer, D.P., 2009. Precision of cerebrovascular reactivity assessment with use of different quantification methods for hypercapnia functional MR imaging. AJNR Am. J. Neuroradiol. 30, 972–977.

Graham, G.D., Zhong, J., Petroff, O.A., Constable, R.T., Prichard, J.W., Gore, J.C., 1994. BOLD MRI monitoring of changes in cerebral perfusion induced by acetazolamide and hypercarbia in the rat. Magn. Reson. Med. 31, 557–560.

Griswold, M.A., Jakob, P.M., Heidemann, R.M., Nittka, M., Jellus, V., Wang, J., Kiefer, B., Haase, A., 2002. Generalized autocalibrating partially parallel acquisitions (GRAPPA). Magn. Reson. Med. 47, 1202–1210.

Hattori, N., Bergsneider, M., Wu, H.M., Glenn, T.C., Vespa, P.M., Hovda, D.A., Phelps, M.E., Huang, S.C., 2004. Accuracy of a method using short inhalation of (15)O-O(2) for measuring cerebral oxygen extraction fraction with PET in healthy humans. J. Nucl. Med. 45, 765–770.

Hino, J.K., Short, B.L., Rais-Bahrami, K., Seale, W.R., 2000. Cerebral blood flow and metabolism during and after prolonged hypercapnia in newborn lambs. Crit. Care Med. 28, 3505–3510.

Hoge, R.D., Atkinson, J., Gill, B., Crelier, G.R., Marrett, S., Pike, G.B., 1999a. Investigation of BOLD signal dependence on cerebral blood flow and oxygen consumption: the deoxyhemoglobin dilution model. Magn. Reson. Med. 42, 849–863.

Hoge, R.D., Atkinson, J., Gill, B., Crelier, G.R., Marrett, S., Pike, G.B., 1999b. Linear coupling between cerebral blood flow and oxygen consumption in activated human cortex. Proc. Natl. Acad. Sci. U. S. A. 96, 9403–9408.

Horvath, I., Sandor, N.T., Ruttner, Z., McLaughlin, A.C., 1994. Role of nitric oxide in regulating cerebrocortical oxygen consumption and blood flow during hypercapnia. J. Cereb. Blood Flow Metab. 14, 503–509.

Ibaraki, M., Miura, S., Shimosegawa, E., Sugawara, S., Mizuta, T., Ishikawa, A., Amano, M., 2008. Quantification of cerebral blood flow and oxygen metabolism with 3-dimensional PET and 15O: validation by comparison with 2-dimensional PET. J. Nucl. Med. 49, 50–59.

Ibaraki, M., Shinohara, Y., Nakamura, K., Miura, S., Kinoshita, F., Kinoshita, T., 2010. Interindividual variations of cerebral blood flow, oxygen delivery, and metabolism in relation to hemoglobin concentration measured by positron emission tomography in humans. J. Cereb. Blood Flow Metab. 30, 1296–1305.

Ishii, K., Sasaki, M., Kitagaki, H., Sakamoto, S., Yamaji, S., Maeda, K., 1996. Regional difference in cerebral blood flow and oxidative metabolism in human cortex. J. Nucl. Med. 37, 1086–1088.

Ito, H., Ibaraki, M., Kanno, I., Fukuda, H., Miura, S., 2005. Changes in cerebral blood flow and cerebral oxygen metabolism during neural activation measured by positron emission tomography: comparison with blood oxygenation level-dependent contrast measured by functional magnetic resonance imaging. J. Cereb. Blood Flow Metab. 25, 371–377.

Ito, H., Kanno, I., Ibaraki, M., Suhara, T., Miura, S., 2008. Relationship between baseline cerebral blood flow and vascular responses to changes in PaCO2 measured by positron emission tomography in humans: implication of inter-individual variations of cerebral vascular tone. Acta Physiol. (Oxf.) 193, 325–330.

Jenkinson, M., Bannister, P., Brady, M., Smith, S., 2002. Improved optimization for the robust and accurate linear registration and motion correction of brain images. Neuroimage 17, 825–841.

Jenkinson, M., Smith, S., 2001. A global optimisation method for robust affine registration of brain images. Med. Image Anal. 5, 143–156.

Jimura, K., Braver, T.S., 2010. Age-related shifts in brain activity dynamics during task switching. Cereb. Cortex 20, 1420–1431.

Jones, M., Berwick, J., Hewson-Stoate, N., Gias, C., Mayhew, J., 2005. The effect of hypercapnia on the neural and hemodynamic responses to somatosensory stimulation. Neuroimage 27, 609–623.

Kruger, G., Glover, G.H., 2001. Physiological noise in oxygenation-sensitive magnetic resonance imaging. Magn. Reson. Med. 46, 631–637.

Langenecker, S.A., Nielson, K.A., Rao, S.M., 2004. fMRI of healthy older adults during Stroop interference. Neuroimage 21, 192–200.

Lecrux, C., Hamel, E., 2011. The neurovascular unit in brain function and disease. Acta Physiol. (Oxf.) 203, 47–59.

Leenders, K.L., Perani, D., Lammertsma, A.A., Heather, J.D., Buckingham, P., Healy, M.J., Gibbs, J.M., Wise, R.J., Hatazawa, J., Herold, S., Beaney, R.P., Brooks, D.J., Spinks, S., Rhodes, C., Frackowiak, R.S.J., 1990. Cerebral blood flow, blood volume and oxygen utilization. Normal values and effect of age. Brain 113, 27–47.

Leung, H.C., Skudlarski, P., Gatenby, J.C., Peterson, B.S., Gore, J.C., 2000. An event-related functional MRI study of the stroop color word interference task. Cereb. Cortex 10, 552–560.

Li, S.C., Sikstrom, S., 2002. Integrative neurocomputational perspectives on cognitive aging, neuromodulation, and representation. Neurosci. Biobehav. Rev. 26, 795–808.

Liu, T.T., Wong, E.C., 2005. A signal processing model for arterial spin labeling functional MRI. Neuroimage 24, 207–215.

Logothetis, N.K., Pauls, J., Augath, M., Trinath, T., Oeltermann, A., 2001. Neurophysiological investigation of the basis of the fMRI signal. Nature 412, 150–157.

Lu, H., Xu, F., Rodrigue, K.M., Kennedy, K.M., Cheng, Y., Flicker, B., Hebrank, A.C., Uh, J., Park, D.C., 2011. Alterations in cerebral metabolic rate and blood supply across the adult lifespan. Cereb. Cortex 21, 1426–1434.

MacDonald, 3rd, A.W., Cohen, J.D., Stenger, V.A., Carter, C.S., 2000. Dissociating the role of the dorsolateral prefrontal and anterior cingulate cortex in cognitive control. Science 288, 1835–1838.

Magri, C., Schridde, U., Murayama, Y., Panzeri, S., Logothetis, N.K., 2012. The amplitude and timing of the BOLD signal reflects the relationship between local field potential power at different frequencies. J. Neurosci. 32, 1395–1407.

Mandell, D.M., Han, J.S., Poublanc, J., Crawley, A.P., Stainsby, J.A., Fisher, J.A., Mikulis, D.J., 2008. Mapping cerebrovascular reactivity using blood oxygen level-dependent MRI in patients with arterial steno-occlusive disease: comparison with arterial spin labeling MRI. Stroke 39, 2021–2028.

Marchal, G., Rioux, P., Petit-Taboue, M.C., Sette, G., Travere, J.M., Le Poec, C., Courtheoux, P., Derlon, J.M., Baron, J.C., 1992. Regional cerebral oxygen consumption, blood flow, and blood volume in healthy human aging. Arch. Neurol. 49, 1013–1020.

Mark, C.I., Slessarev, M., Ito, S., Han, J., Fisher, J.A., Pike, G.B., 2010. Precise control of end-tidal carbon dioxide and oxygen improves BOLD and ASL cerebrovascular reactivity measures. Magn. Reson. Med. 64, 749–756.

McPherson, R.W., Derrer, S.A., Traystman, R.J., 1991. Changes in cerebral CO2 responsivity over time during isoflurane anesthesia in the dog. J. Neurosurg. Anesthesiol 3, 12–19.

Milham, M.P., Erickson, K.I., Banich, M.T., Kramer, A.F., Webb, A., Wszalek, T., Cohen, N.J., 2002. Attentional control in the aging brain: insights from an fMRI study of the stroop task. Brain Cogn. 49, 277–296.

Mintun, M.A., Vlassenko, A.G., Shulman, G.L., Snyder, A.Z., 2002. Time-related increase of oxygen utilization in continuously activated human visual cortex. Neuroimage 16, 531–537.

Mohtasib, R.S., Lumley, G., Goodwin, J.A., Emsley, H.C., Sluming, V., Parkes, L.M., 2012. Calibrated fMRI during a cognitive Stroop task reveals reduced metabolic response with increasing age. Neuroimage 59, 1143–1151.

O'Rourke, M.F., Hashimoto, J., 2007. Mechanical factors in arterial aging: a clinical perspective. J. Am. Coll. Cardiol. 50, 1–13.

Park, D.C., Reuter-Lorenz, P., 2009. The adaptive brain: aging and neurocognitive scaffolding. Annu. Rev. Psychol. 60, 173–196.

Prakash, R.S., Voss, M.W., Erickson, K.I., Lewis, J.M., Chaddock, L., Malkowski, E., Alves, H., Kim, J., Szabo, A., White, S.M., Wojcicki, T.R., Klamm, E.L., McAuley, E., Kramer, A.F., 2011. Cardiorespiratory fitness and attentional control in the aging brain. Front. Hum. Neurosci. 4, 229.

Reitan, R.M., 1958. Validity of the Trail Making Test as an indicator of organic brain damage. Perceptual and Motor Skills 8, 271–276.

Reuter-Lorenz, P.A., Cappell, K.A., 2008. Neurocognitive aging and the compensation hypothesis. Curr. Direct. Psychol. Sci. 17, 177–182.

Reuter-Lorenz, P.A., Park, D.C., 2010. Human neuroscience and the aging mind: a new look at old problems. J. Gerontol. B Psychol. Sci. Soc. Sci. 65, 405–415.

Salat, D.H., Buckner, R.L., Snyder, A.Z., Greve, D.N., Desikan, R.S., Busa, E., Morris, J.C., Dale, A.M., Fischl, B., 2004. Thinning of the cerebral cortex in aging. Cereb. Cortex 14, 721–730.

Samanez-Larkin, G.R., D'Esposito, M., 2008. Group comparisons: imaging the aging brain. Soc. Cogn. Affect. Neurosci. 3, 290–297.

Schneider-Garces, N.J., Gordon, B.A., Brumback-Peltz, C.R., Shin, E., Lee, Y., Sutton, B.P., Maclin, E.L., Gratton, G., Fabiani, M., 2010. Span, CRUNCH, and beyond: working memory capacity and the aging brain. J. Cogn. Neurosci. 22, 655–669.

Shmuel, A., Yacoub, E., Pfeuffer, J., Van de Moortele, P.F., Adriany, G., Hu, X., Ugurbil, K., 2002. Sustained negative BOLD, blood flow and oxygen consumption response and its coupling to the positive response in the human brain. Neuron 36, 1195–1210.

Slessarev, M., Han, J., Mardimae, A., Prisman, E., Preiss, D., Volgyesi, G., Ansel, C., Duffin, J., Fisher, J.A., 2007. Prospective targeting and control of end-tidal CO2 and O2 concentrations. J. Physiol. 581, 1207–1219.

Smith, S.M., 2002. Fast robust automated brain extraction. Hum. Brain Mapp. 17, 143–155.

Sonntag, W.E., Lynch, C.D., Cooney, P.T., Hutchins, P.M., 1997. Decreases in cerebral microvasculature with age are associated with the decline in growth hormone and insulin-like growth factor 1. Endocrinology 138, 3515–3520.

Stefanovic, B., Warnking, J.M., Rylander, K.M., Pike, G.B., 2006. The effect of global cerebral vasodilation on focal activation hemodynamics. Neuroimage 30, 726–734.

Tancredi, F.B., Gauthier, C.J., Madjar, C., Bolar, D.S., Fisher, J.A., Wang, D.J., Hoge, R.D., 2012. Comparison of pulsed and pseudocontinuous arterial spin-labeling for measuring CO(2) -induced cerebrovascular reactivity. J. Magn. Reson. Imaging 36, 312–321.

Triantafyllou, C., Hoge, R.D., Krueger, G., Wiggins, C.J., Potthast, A., Wiggins, G.C., Wald, L.L., 2005. Comparison of physiological noise at 1.5 T, 3 T and 7 T and optimization of fMRI acquisition parameters. Neuroimage 26, 243–250.

Wahlund, L.O., Barkhof, F., Fazekas, F., Bronge, L., Augustin, M., Sjogren, M., Wallin, A., Ader, H., Leys, D., Pantoni, L., Pasquier, F., Erkinjuntti, T., Scheltens, P., 2001. A new rating scale for age-related white matter changes applicable to MRI and CT. Stroke 32, 1318–1322.

Wang, J., Aguirre, G.K., Kimberg, D.Y., Roc, A.C., Li, L., Detre, J.A., 2003. Arterial spin labeling perfusion fMRI with very low task frequency. Magn. Reson. Med. 49, 796–802.

Wasylyshyn, C., Verhaeghen, P., Sliwinski, M.J., 2011. Aging and task switching: a meta-analysis. Psychol. Aging 26, 15–20.

Wechsler, D., 1997. WAIS-III Administration and Scoring Manual. The Psychological Corporation.

Williams, D.S., Detre, J.A., Leigh, J.S., Koretsky, A.P., 1992. Magnetic resonance imaging of perfusion using spin inversion of arterial water. Proc. Natl. Acad. Sci. U. S. A. 89, 212–216.

Woolrich, M., 2008. Robust group analysis using outlier inference. Neuroimage 41, 286–301.

Woolrich, M.W., Behrens, T.E., Beckmann, C.F., Jenkinson, M., Smith, S.M., 2004. Multilevel linear modelling for FMRI group analysis using Bayesian inference. Neuroimage 21, 1732–1747.

Woolrich, M.W., Ripley, B.D., Brady, M., Smith, S.M., 2001. Temporal autocorrelation in univariate linear modeling of FMRI data. Neuroimage 14, 1370–1386.

Wu, W.C., Fernandez-Seara, M., Detre, J.A., Wehrli, F.W., Wang, J., 2007. A theoretical and experimental investigation of the tagging efficiency of pseudocontinuous arterial spin labeling. Magn. Reson. Med. 58, 1020–1027.

Xu, F., Uh, J., Brier, M.R., Hart, Jr., J., Yezhuvath, U.S., Gu, H., Yang, Y., Lu, H., 2011. The influence of carbon dioxide on brain activity and metabolism in conscious humans. J. Cereb. Blood Flow Metab. 31, 58–67.

Yamauchi, H., Okazawa, H., Kishibe, Y., Sugimoto, K., Takahashi, M., 2002. Changes in blood flow and oxygen metabolism during visual stimulation in carotid artery disease: effect of baseline perfusion and oxygen metabolism. Stroke 33, 1294–1300.

Yamaguchi, T., Kanno, I., Uemura, K., Shishido, F., Inugami, A., Ogawa, T., Murakami, M., Suzuki, K., 1986. Reduction in regional cerebral metabolic rate of oxygen during human aging. Stroke 17, 1220–1228.

Yeung, N., Nystrom, L.E., Aronson, J.A., Cohen, J.D., 2006. Between-task competition and cognitive control in task switching. J. Neurosci. 26, 1429–1438.

Yun, J.Y., Lee, D.Y., Seo, E.H., Choo, I.H., Park, S.Y., Kim, S.G., Woo, J.I., 2011. Neural correlates of stroop performance in Alzheimer's disease: a FDG-PET study. Dement. Geriatr. Cogn. Dis. Extra 1, 190–201.

Zappe, A.C., Uludag, K., Oeltermann, A., Ugurbil, K., Logothetis, N.K., 2008. The influence of moderate hypercapnia on neural activity in the anesthetized nonhuman primate. Cereb. Cortex 18, 2666–2673.

Zhang, Y., Brady, M., Smith, S., 2001. Segmentation of brain MR images through a hidden Markov random field model and the expectation-maximization algorithm. IEEE Trans Med. Imaging 20, 45–57.

Zysset, S., Schroeter, M.L., Neumann, J., von Cramon, D.Y., 2007. Stroop interference, hemodynamic response and aging: an event-related fMRI study. Neurobiol. Aging 28, 937–946.